EVALUATION OF THE CURRENT MODELS OF DARK ENERGY

D. Burrow, L. Butcher, M. Gornall, A. Taylor and **R. Unnikrishnan.**

Lancaster University
Department of Physics
Beta Collaboration

March 2019

Abstract

We aimed to determine the range of $\Omega_{\Lambda,0}$ values necessary to solve the age problem of the universe. This was found to be approximately $0.58 < \Omega_{\Lambda,0} < 0.77$ in the $1-\sigma$ limit (to 2 significant figures). Further to this, we investigated the value of age of the universe for a range of ω_X values that was $-0.5 < \omega_X < -15$. We evaluated whether the ESA EUCLID mission will be able to distinguish between ω_a and ω_p values of simulated dark energy (DE) values and those of the ΛCDM model. We found values of $\omega_a = 0.112$ and $\omega_p = -0.973$ and determined EUCLID will be able to distinguish these from the ΛCDM model. As well as the EUCLID mission, we evaluated whether NASA's WFIRST telescope will be able to distinguish between the ΛCDM model and two other models of DE, Scaling Freezing Quintessence (SFQ) and modified gravity. We tested 2 different models of SFQ, we found that WFIRST could distinguish SFQ 1 from ΛCDM to $1-\sigma$ and $2-\sigma$ errors, it could not distinguish SFQ 2 for any error range and finally that it could distinguish modified gravity from ΛCDM for both $1-\sigma$ and $2-\sigma$ error ranges.

Contents

1 INTRODUCTION

The discovery that the expansion of the universe is accelerating at present has transformed the field of cosmology and initiated the somewhat problematic and, as yet, unsuccessful search for the mysterious substance known as dark energy (DE), which will hopefully explain this observation. It is thought that DE accounts for $\sim 70\%$ of the overall energy density of our universe [11] at present and yet we have never directly observed it, we have only seen evidence that it should exist, such as Baryon Acoustic Oscillations (BAO) or the age problem, which will be discussed in sections 2.2.2 and 2.1.2 of this report, respectively. DE is described by it's equation of state, $\omega_X = P/\rho$, where ω_X is the DE barotropic parameter, which should be less than $-1/3$ in order for the theory to match with observation.

Over the course of the next few years, there will be several missions launched to try and measure the properties of DE and hopefully shine light on its origins. Examples of such missions are the ESA EUCLID telescope and NASA's WFIRST project, which will be summarised in sections 2.2.4 and 2.2.5 respectively. The primary objective of both of these missions is to determine the equation of state of DE and whether it has a time dependence, which would explain why the expansion rate of the universe seems to have changed over cosmic history. Further on in the report, we will also evaluate whether EUCLID and WFIRST will be able to distinguish between the various different models of DE, in order to determine which one describes it properly, the details of this can be found in section 4. Provided these missions are successful, we could confirm the existence of DE within the next decade, a discovery which may help us understand some of the most fundamental questions about our universe.

We would also like to understand what DE actually is, i.e. how to describe it physically. With regards to this there are a few different theories, the most simple of these is that DE is described by a cosmological constant Λ, this is know as the ΛCDM model. The ΛCDM model is characterised by an equation of state with $\omega_\Lambda = -1$, however we find that the energy scales of the universe under the cosmological constant description of DE are much larger than the observed ones. Therefore it seems that we need to find a different characterisation of DE. There are two popular theories which could solve this problem:

1. **Quintessence** - DE is a canonical scalar field, which is minimally coupled to gravity [12].
2. **Modified Gravity** - The idea that our current theory of general relativity doesn't apply on the scales of the universe and thus needs to be changed This is discussed in section 2.3.1 of this report.

Quintessence in itself provides various different models that describe DE in different way. These can be classified into 2 categories: thawing and freezing. In this report we will focus on the freezing model of quintessence, more specifically on the scaling freezing quintessence (SFQ). The full analysis of SFQ can be found in section 2.2.1.

This report will investigate and discuss three distinct ideas behind DE. First we will look into the direct evidence of DE, before examining future probes of DE and how future satellite missions will help us determine its nature. Finally, we will discuss an alternative theory to DE known as Modified Gravity.

2 THEORY

2.1 Direct evidence of dark energy

Included in this section is a discussion of one of the key pieces of evidence for DE, known as "the age problem". First there is a description of how we obtain the current age of the universe, from looking at the oldest observable stars, followed by an explanation of the age problem and how it serves as evidence for DE. Finally, a summary of the method used to find the observational range of $\Omega_{m,0}$, which gives the total mass density of normal matter.

2.1.1 Determining the age of the universe

A white dwarf is formed from a small to medium mass star, similar to the size of the sun. It forms when the main sequence star has used up all its central nuclear fuel and expels its outer layers as a planetary nebula. This leaves a very dense star, approximately the size of a planet. They are very hot at the beginning, but they will cool down after time into a black dwarf. As a white dwarf cools, its size does not change, hence the cooling rate is only dependent on temperature; once the star starts to cool the rate of cooling decreases dramatically. The coolest and faintest white dwarfs are the oldest, so if we know the temperature and luminosity we can determine the size of the white dwarf and thus we can calculate the cooling rate. From this you can work backwards and estimate how old the white dwarf is [1]. Now if we were to find a globular cluster of white dwarfs, we can estimate the age of the cluster by using the techniques mentioned previously. Globular clusters are formed from huge molecular clouds, as these clouds collapse new stars are born; this process takes roughly 1 billion years [2]. Globular clusters are used for age determination as there is less free gas available at present, thus implying that these clusters would have to have formed in the early universe. There are many generations of stars in the cluster, however the subsequent generations evolve from the previous ones. This results in the age difference between the various generations of stars in the cluster being less than 1% of the clusters age [2]. As well as this, the stars in the cluster are at the same distance and so have the same reddening. In many of the white dwarf globular clusters the white dwarf stars have been estimated to be around 12-13 billion years old. From this fact, an accurate estimate of the age of the universe would be around 13-14 billion years old [3]

2.1.2 The age problem in the universe

The age problem of the universe arose when scientists were trying to calculate the age of distant stars. When comparing their findings with the age of universe, determined via the globular cluster method (section 2.1.1), it appeared that the stars were older than the universe itself, thus they would have formed before the Big Bang. At first this caused considerable confusion as no one knew whether it was the age of the universe that had been incorrectly calculated, or the age of the stars. This problem also resonated when finding the size of the observable universe, calculated to be around 46 Glyrs, which is huge in comparison to the age of the universe, a mere 13.8 Gyrs. Eventually it was determined that the solution to this problem is expansion. Expansion which is thought be caused by DE. The accelerated expansion of the universe is most prevalent when observing galaxies, which shows that the further away the galaxy is, the faster it is actually moving away from us. This supports the existence of DE.[16]

2.1.3 Observational range of $\Omega_{m,0}$

To estimate the range of total mass density in the universe it is best to apply a constraint on the total density of clustered matter. Which will come from a combination of X-Ray measurements of clusters and large hydrodynamic simulations. The X-Rays coming from the hot gas which dominates the the total baryon fraction in clusters are measured for temperature and luminosity, these are then inverted. This is done so by assuming hydro-static equilibrium of gas in the clusters, and using this we can obtain the gravitational potential for the system. From that we can obtain the ratio of baryon to total mass of system. Then through applying a constraint on the total baryon density of the universe coming from the BBN as well as assuming that galaxy clusters give a fair estimate of the total clustered mass in the universe we can obtain the range for total observed mass density in the universe[13]. Which is as follows.

$$\Omega_{m,0} = 0.35 \pm 0.1, \tag{2.1}$$

Using this we can plot the bounds onto a graph, to find the $1-\sigma$ and the $2-\sigma$ bounds of different ω_X.

2.2 Determining the nature of dark energy

This section examines some of the work that will be done in the near future, to probe the universe and find out more about the origins and evolution of DE. Initially there is a discussion of the theoretical principles that describe DE, that are to be investigated. Afterwards there are summaries of the missions that will be launched in the coming years to conduct these investigations.

2.2.1 The SFQ model

The most simple candidate for dark energy is a cosmological constant, Λ, which has an equation of state that gives $\omega_\Lambda = -1$ at all times. However we find that the observed energy scales for dark energy do not agree with those predicted by the cosmological constant [11]. A more suitable choice for dark energy is the scaling freezing quintessence model (or SFQ), which is a canonical scalar field, ϕ, that describes the accelerated expansion of the universe in later times. The equation of state of this model evolves with time and the value of ω at a time given by the scale factor, a, is[12]:

$$\omega(a) = -1 + \frac{1}{1 + (\frac{a}{a_t})^{1/\tau}}, \tag{2.2}$$

where a_t is the value of the scale factor at transition where scaling behaviour ends and τ is the transition width ($\tau \sim 0.33$) is an appropriate choice for analytical expression to agree with the numerical one [12]. We can see, simply by the definition of this equation of state, that $\omega(a) \geq -1$ at all times, which satisfies the constraints on the density parameter of DE.

The dynamics of any quintessence model is described by its scalar potential. Specifically the SFQ model has a potential of the form [12]:

$$V(\phi) = V_1 e^{-\lambda_1 \phi / M_{pl}} + V_2 e^{-\lambda_2 \phi / M_{pl}}, \tag{2.3}$$

where $\lambda_1 >> 1$, $\lambda_2 << 1$, V_1 and V_2 are constants and M_{pl} is the Planck mass. This implies that at early times, the λ_1 term dominates and solutions scale with matter; whereas at later times λ_2 dominates, thus we have dark energy domination and accelerated expansion.

2.2.2 BAO background theory

Baryon Acoustic Oscillations (BAO) are patterns imprinted in the clustering of galaxies that provide a standard ruler to measure the expansion of the universe. The properties of the patterns are derived from the measurements of distances to galaxies. A BAO is formed from a single perturbation of plasma which is uniform except for at the origin where there is an excess of matter made up of baryons (electrons and protons), photons and dark matter (DM) [4]. High pressures from the photon-matter interactions creates vast amounts of outward pressure. The resulting counteracting forces of gravity and this pressure drives the baryon-photon fluid outwards together at relativistic speeds in a spherical shell from the origin as a sound wave. This expansion continues for around 10^5 years [5]. After this time the baryons have cooled enough to allow the electrons and protons to form together to create hydrogen and the photons then decouple from the baryons and diffuse away becoming almost completely uniform whilst the baryons remain at a fixed radius around 500 million light years from the origin, also known as the sound horizon [5]. The baryons now only interact gravitationally with the dark matter centre and therefore some of the baryons are drawn towards the origin, this leaves us with over-densities of matter at both the origin and the shell at the sound horizon [5]. Therefore the distribution of galaxies form a pattern of a cluster of galaxies in the centre of a spherical shell of galaxies at the sound horizon as shown in figure 1. Meaning that if you pick a galaxy, at random, in the Universe, you are more likely to find a second galaxy at a distance of 500 million light years than you are to find a second galaxy at any other distance (300 or 400 million light years for example).

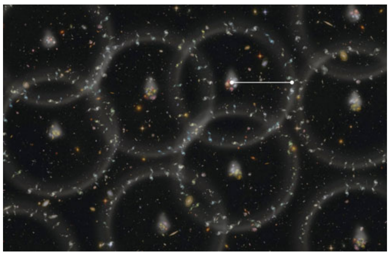

Figure 1: Cartoon image produced by the BOSS project showing the spheres of baryons around initial dark matter clumps [14].

2.2.3 Defining luminosity distance, d_l, and its relation to $d(z)$ in an expanding universe

As the light flux for a star travels a distance and reaches an observer it is reduced by the area as

$$F = \frac{L}{4\pi {d_l}^2}, \tag{2.4}$$

where F is the flux at observer, L is the absolute luminosity, and d_L is the luminosity distance.
The relation for luminosity distance can be related to the physical distance by

$$F = \frac{1}{(1+z)^2} \frac{L}{4\pi d(z)^2}, \tag{2.5}$$

$$(1+z)d(z) = \sqrt{\frac{L}{4\pi F}}, \tag{2.6}$$

the RHS of this equation can be represented as d_L,

$$d_l = (1+z)d(z), \tag{2.7}$$

The $(1+z)$ factor comes from both the redshift reducing the energy of the photons and increasing the time difference between arrivals[10]. So essentially, as the expansion increases the redshift increases and so you will need a term to account for this when measuring distances and this is what the $(1+z)$

factor does [9].

2.2.4 The EUCLID mission

The EUCLID mission was conceived by the European Space Agency (ESA) to answer some of the biggest questions in modern cosmology, which it will achieve by measuring weak gravitational lensing (WL) and baryonic acoustic oscillations (BAO is discussed in section 2.2.2). EUCLID (the telescope itself) is set to be launched in June 2022 [7] and will carry out two surveys [8]:

- **Wide survey** - covering an area of $15000° - 20000°$.
- **Deep survey** - over an area of $\sim 40°$ and up to red shifts of $z \sim 8$.

By completing these surveys, EUCLID will map the large scale structure of the universe over a cosmic time covering the last 10 billion years. Hopefully taking these measurements will enable the EUCLID mission to achieve it's main scientific objectives, one of which is to reach a Dark Energy figure of merit (FoM)> 400, using WL and galaxy clustering; this FoM roughly corresponds to a $1-\sigma$ error for w_p and w_a of 0.02 and 0.1 respectively [8]. On top of this, the mission aims to find a value for the exponent of the universal growth factor, γ, with a $1-\sigma$ precision of < 0.02, which will be sufficient to distinguish between General Relativity and any modified-gravity theories, as explanations for the accelerated expansion of the universe.

The payload of the mission (i.e. the telescope) will be a Korsch telescope with an aperture size of 1.2m. This telescope consists of two instruments: a visual instrument (VIS) and a near infrared instrument (NISP) [8]. VIS will focus on weak lensing measurements, it contains 36 CCD's and will measure the shape of galaxies with a resolution $< 0.2''$. Whereas NISP has 3 near infrared (NIR) bands (Y,J,H) and uses 16 NIR detectors with $0.3''$ pixels.

2.2.5 WFIRST mission summary

The WFIRST mission is an orbital space telescope that will attempt to test and answer a wide range of theories and questions relating to the cosmos. These being the testing of a range of dark energy models in addition to the further surveying of exoplanets and determination of large scale cosmic structure.

For this to be accomplished it is equipped with a $2.4m$ diameter aperture telescope that is capable of both wide field imaging and slit less spectroscopy, as well as containing a coronograph to aide with the exoplanet survey. Allowing the mission to conduct deep field imaging as well as identify planets with small orbital radii. Furthermore, the main structure has been altered to support a three mirror system, as opposed to a two mirror one, as well as the addition of thermal blankets to lower its operating temperature to $270K$ improving its efficiency in the infrared range [15].

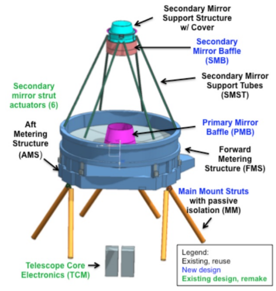

Figure 2: Diagram showing some of the proposed modification to the WFIRST telescope [15].

To test a range of dark energy theories the WFIRST mission will make several distance measurements using various methods. These include measuring galaxy clustering as well as using BAO as a standard length to determine physical distance much like the EUCLID mission. However, the method considered in this report is the measurement of luminosity distances through using type1a supernova as standard candles. The aggregate precision of these measurements being dependent upon the redshift they are taken at with at $Z = 0.50$ and $Z = 1.32$ having precision's of 0.20% and 0.34% respectively. Through comparing these measured distances with what would be expected for the different models, it may be possible to determine which of them is likely to be correct [15].

With regards to the other aims, by continuing to observe exoplanets it may be possible to create a statistical census of the different planet types and their orbital radii, as well as identifying planets close to their parent star using the coronograph. In addition, by conducting a high latitude survey it will be possible to determine cosmic structure shortly after the big bang it may be possible to further understand large scale structure formation and how well they match current models [15].

2.3 An alternative to dark energy

2.3.1 The theory behind the modified gravity model

The modified gravity model is an alternative model to explain the behaviours of the late-time universe, as opposed to using the cosmological constant. The theory utilises the knowledge that there are extra dimensions, above those that we can observe, and that these dimensions have an infinite volume, into which there is a gravity leakage from our own. We know if general relativity is conserved then you can explain the accelerating universe through the existence of dark energy and the fact that there is a cosmological constant. However, if general relativity is not conserved then models such as modified gravity can be implemented to solve and fix the breaking down of the Friedmann equation. The data from a report, written by G.Dvali and M.S.Turner on Dark Energy as a Modification of

The Friedmann Equation [6], suggests a recent period of acceleration ($z \leq 0.5$) preceding an earlier period of deceleration ($z \geq 0.5$). Thus, allowing for modified dynamics cannot solely eliminate the phenomenon of accelerated expansion; hence if these extra dimensions are present then we will need to consider modifying the Friedmann equation. This will involve the addition of the term, $((1-\Omega m)H^{\alpha})/(H^{\alpha-2})$, which will cater for the idea that there exists extra dimensions into which the gravity from the dimensions in our universe leaks into. This means the gravitational influences in our universe are affected, becoming weaker. In order for this behaviour to occur the extra dimension must have an infinite volume, thus at short distances (early times) the gravitational dynamics are very close to 4D Einstein gravity, but at long distances the laws of gravity will be modified. So the modified gravity allows universe to become self accelerated and the extra dimensions leads to a modified term which transforms the Friedmann equation into the following

$$H^2 \pm \frac{H}{r_c} = \frac{8\pi G \rho_m}{3}, \tag{2.8}$$

where the r_c term represents the crossover point from 4D Einstein gravity to 5D Einstein gravity. 5D is important when H is small and z is small, so in early times H is high and r_c is irrelevant. Furthermore r_c is stable under quantum corrections whilst the cosmological constant is not. Due to this, the modified gravity theory may have a higher potential than the cosmological constant model.

3 METHOD

3.1 Examining the direct evidence of DE

Here we will derive the key results for measuring and calculating the direct evidence for dark energy, as well as outlining the coding method used to determine the age of the universe at various values of ω_X.

3.1.1 Derivation of t_0 as a function of $\Omega_{\Lambda,0}$

Starting with the Friedmann equation for the case of a flat universe we will derive the equation for the age of the universe at present time,

$$H^2 = \left(\frac{\dot{a}}{a}\right)^2 = \frac{8\pi G \rho_c}{3}. \tag{3.1}$$

By considering this equation at present time and manipulating it appropriately, we can show that the final result for the age of the universe at present is,

$$t_0 = \frac{2}{3}\frac{H_0^{-1}}{\sqrt{\Omega_{\Lambda,0}}}\ln\left[\frac{1+\sqrt{\Omega_{\Lambda,0}}}{\sqrt{1-\Omega_{\Lambda,0}}}\right]. \tag{3.2}$$

For the full derivation see appendix A.1.

3.1.2 Derivation of t_0 as a function of $\Omega_{m,0}$ for different ω_X

Here we will obtain the expression for t_0 as a function of $\Omega_{m,0}$ for different ω_X. This expression contains an integral that will need to be numerically integrated. We will start by using equation 3.3 for the case where ρ_Λ is replaced by $\rho_X(a)$, where the a dependence of $\rho_X(a)$ is determined by ω_X.

$$\int_0^a \frac{1}{a\sqrt{\rho_m+\rho_\Lambda}}da = \int_0^t \sqrt{\frac{8\pi G}{3}}dt, \tag{3.3}$$

by applying several steps (Appendix A.2), we reach the final expression,

$$t_0 = \frac{2}{3}\frac{1}{\Omega_{m,0}^{\frac{1}{2}}H_0}. \tag{3.4}$$

Thus we have derived the upper bound on t_0 as a function of $\Omega_{m,0}$ when $\omega_X \to -\infty$.

3.1.3 Method of determining the age of the universe in terms of ω_X and $\Omega_{m,0}$

In the case of where the dark energy density is no longer constant and is instead dependant on the scale factor (as shown in section 3.1.2), it is no longer possible to determine the value of the integration analytically. Therefore, it is necessary to use numerical integration to find the value of the age of the universe for the combination of different ω_x and $\Omega_{m,0}$ values.

To calculate this age, a value of ω_x is inputted by the user and the value of the integration is calculated for different values of $\Omega_{m,0}$, increasing by 0.01 with each iteration, up to a maximum of 1. As for the case of a flat universe the total value of the density parameters will equal 1, thus it becomes possible to determine the $\Omega_{x,0}$ value and subsequently their respective present day matter densities. In this case the method used for the numerical integration is the trapezium method given in the general form,

$$h = \frac{b-a}{N} \qquad \int_a^b f(x)dx = h\left(\frac{1}{2}(f(a)+f(b)) + \sum_{i=1}^{N-1} f(a+ih)\right). \tag{3.5}$$

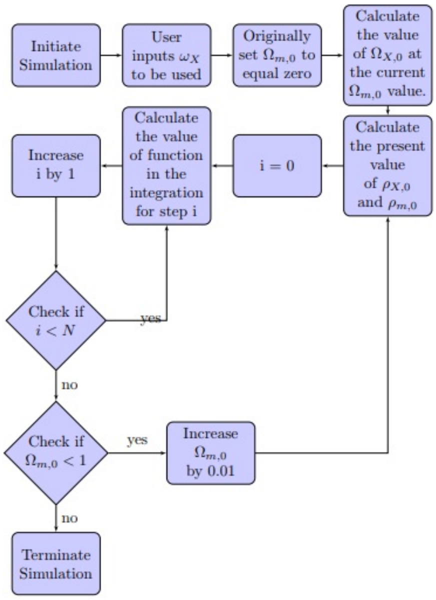

Figure 3: Flowchart showing the progression through the code used to calculate the universe age for different ω_X values.

Utilising this method, it is possible to determine the age of the universe for a variety of ω_x values, given that the present energy densities can be calculated for both matter and dark energy.

Furthermore, from examining the curves for the different ω_x values, the one that corresponds to the intersections of the $1-\sigma$ and $2-\sigma$ upper and lower bounds for the age of the universe and present matter density parameter, can be determined. This largely being done by a modified version of the code where the t_0 and $\Omega_{m,o}$ values are inputted and the ω_x value that gives the smallest difference between calculated and given t_0 values is produced.

3.2 Methods of determining the nature of dark energy

This section outlines how future experiments will probe the properties of DE. All of the necessary set up, in terms of calculation and derivations, are included in the subsequent subsections, followed by a description of the practical steps taken to evaluate our understanding of DE. We also outline how the WFIRST mission will distinguish between various DE models.

3.2.1 Preliminary calculations

In order to find the physical distance as a function of redshift it is first necessary to consider to different physical distance relations,

$$dr = cdt \quad \text{and} \quad dr = a(t)dX. \tag{3.6}$$

Through the use of these equations and several additional steps it is possible to show that,

$$d(z) = a_0 \int_{a(z)}^{a_0} \frac{c}{a^2 \sqrt{\frac{8\pi G}{3}} \left(\left(\frac{a_0}{a}\right)^3 \rho_{m,0} + e^{-\int_{a_0}^{a(z)} \frac{3(1+\omega_X(a))}{a} da} \rho_{x,0} \right)^{1/2}} da. \tag{3.7}$$

This is the equation for physical distance as a function of redshift. The full derivation is shown in appendix B.1.

3.2.2 Derivation of θ_{BAO} in terms of z

If the BAO length at present, l_{BAO}, between two distant objects can be measured, and the physical distance to them from earth, $d(z)$, is known, then it is easy to calculate the angular size of the BAO length, θ_{BAO}, between them. The distances involved in this calculation mean that we can make a few approximations: we know that $d(z) > l_{BAO}$ which means that $\theta_{BAO} << 1$ and hence we will be able to make a small angle approximation, i.e. $\sin(x) \sim x$. Once we have all of this information, it is a case of simple trigonometry to derive θ_{BAO}, as shown in figure 4. From figure 4 we can clearly see that:

$$\sin(\frac{\theta_{BAO}}{2}) = \frac{l_{BAO}/2}{d(z)}, \tag{3.8}$$

so by using the small angle approximation (as detailed above), we can eliminate the sine function and get rid of the factors of 1/2. This gives us:

$$\theta_{BAO} = \frac{l_{BAO}}{d(z)}, \tag{3.9}$$

which is our final equation for θ_{BAO} in terms of redshift, z.

In this derivation we must use the values of l_{BAO} and $d(z)$ in present times. The sources are at a very high redshift ($z > 1$), hence by the time their light reaches us, it is so redshifted that we observe them at their current values of d(z) and separation. Thus these are the values we use.

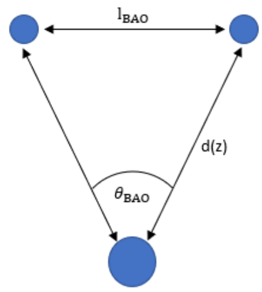

Figure 4: Diagram showing how θ_{BAO}, l_{BAO} and $d(z)$ are related.

3.2.3 Derivation of the CPL parameterization for a flat universe for d(z)

For this derivation we need to show (appendix B.2) that ρ_X can be expressed as:

$$\ln \frac{\rho_X(a)}{\rho_{X,0}} = -\int_{a_0}^{a} \frac{3(1+\omega_X(a))}{a} da, \tag{3.10}$$

and it can be shown that the formula for the CPL Parameterization for a flat universe for d(z) can be expressed in its desired form of:

$$d(z) = \frac{c}{H_0 a_0^{\frac{1}{2}}} \int_{a(z)}^{a_0} \frac{da}{a^{\frac{1}{2}} \left[\Omega_{m,0} + \Omega_{X,0}\left((\frac{a_0}{a})^{3(\omega_p+\omega_a)} e^{-3\omega_a(1-\frac{a}{a_0})} \right)\right]^{\frac{1}{2}}}, \tag{3.11}$$

for the full derivation see the appendix B.2.

3.2.4 Method used to determine ω_p and ω_a

To determine the values of ω_a and ω_p that correspond to the CPL parameterization for the given set of simulated data it was to calculate the value $d(z)$ for a range of different combinations of ω_a and ω_p and compare them with those calculated using equation 3.9.

To gain accurate solutions it was necessary to compare the answers for two different sets of redshift θ_{BAO} combinations as the values of ω_a and ω_p that may give correct answers for one combination may not for the other.

Given that the value of the integration in equation 3.11 could not be done analytically it was again necessary to use numerical integration methods in much the same way as was previously described in section 3.1.3. In order to determine which combination of ω_a and ω_p values where correct it was necessary to run the code through all possible combinations of the values and determine which of these gave the same distance result as that of equation 3.9. This general process being displayed in figure 5. Given that the ω_a and ω_p values are only being determined to 3 decimal places it was decided

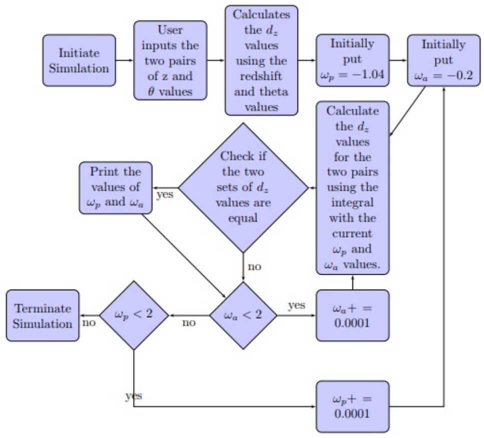

Figure 5: Flowchart displaying the general path through the code used to determine the values of ω_p and ω_a for a given set of simulated data.

that their distance values would only match what was expected to 6 significant figures. In the case of this being true the values of ω_a and ω_p where displayed to the user.

As the values that where being measured against where entered by the user it is possible to use the same simulation for different simulated data sets other than the one used in this report.

3.2.5 Derivation of luminosity distances for the pure matter and cosmological constant universes

We need to determine analytical solutions for the $d(z)$ integration for both the pure cosmological model and the pure matter model. Initially for the pure cosmological model where $w_x = -1$ such that

$$\rho_x = \rho_{x,0} \quad \text{and} \quad \rho_{m,0} = \rho_m = 0, \tag{3.12}$$

this therefore means that $H(a) = H_0$ at all times, so that equation 3.7 may be integrated and applied to equation 2.7 to become,

$$d_L(z) = (1+z)\frac{c}{H_0}\left[-\frac{1}{a}\right]_{a_z}^{1}. \tag{3.13}$$

For the pure matter universe it can instead be said that

$$\rho_x = \rho_{x,0} = 0 \quad \text{and} \quad \rho_m = \left(\frac{1}{a}\right)^3 \rho_{m,0}, \tag{3.14}$$

therefore when this applied to equation 3.7 it may then be integrated and applied to equation 2.7 to become,

$$d_L(z) = (1+z)\left(\frac{8\pi G\rho_{m,0}}{3}\right)^{-\frac{1}{2}} c[2a^{\frac{1}{2}}]^1_{a(z)}. \tag{3.15}$$

3.2.6 Explanation of code and method used to determine luminosity distance

To determine whether WFIRST can distinguish between the different dark energy models from the cosmological constant, it is necessary to calculate the luminosity distance at increasing redshift values for these models. As equation 3.7 could not be solved analytically it was necessary to use numerical integration as previously described in section 3.1.3.

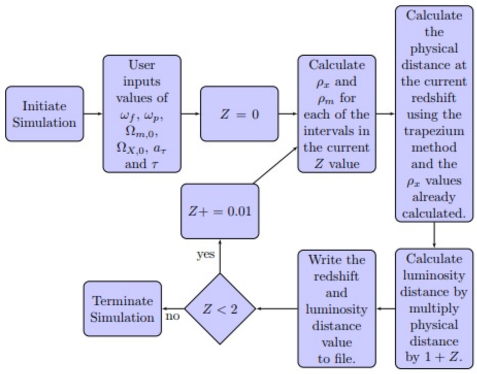

Figure 6: FlowChart showing the general method by which the luminosity distances $d_L(z)$ are calculated for the different dark energy models and the pure matter model.

Equation 3.7 contains a second integration within the main integration for calculating the physical distance; with this inner integration being used to calculate the value of the dark energy density at different redshift values. So before being able to calculate the physical distance at each of the points in its numerical integration, its necessary to calculate the value of the dark energy density using the same numerical integration techniques at those points. Through doing this it is possible to calculate the physical distance, $d(z)$, at different redshifts and relate them to the luminosity distance through equation 2.7. Once these values are known for the different models they may be used to determine whether WFIRST has the capability to distinguish between the different models given the difference in their luminosity distances.

As the different initial parameters are inputted by the user, it is possible to use the same simulation for a variety of different starting conditions. Furthermore, as the calculation of $\omega_x(a)$ is contained within a separate part of the code to the rest of the integral it can be altered for different models without modifying the rest of the code. Which in this case was given by,

$$\omega_X(a) = \omega_f + \frac{\omega_p - \omega_f}{1 + \left(\frac{a}{a_t}\right)^{\frac{1}{\tau}}}. \tag{3.16}$$

3.2.7 Derivation of deceleration parameter

In order to derive the deceleration parameter q in terms of ω_x and Ω_x must first consider the equations,

$$q = -\frac{1}{H^2}\frac{\ddot{a}}{a} \quad \text{and} \quad \frac{\ddot{a}}{a} = -\frac{4\pi G}{3}\left(\rho + \frac{3P}{c^2}\right). \tag{3.17}$$

Through the use of these equations and considering the equation for critical density it can be shown that,

$$q = \frac{1}{2}\left(1 + \frac{3P}{\rho_c c^2}\right). \tag{3.18}$$

As $P = \sum P_i = \sum w_i \rho_i c^2$ and $\omega_m = 0$ so $P = \omega_x \rho_x c^2$ can produce the equation,

$$q = \frac{1}{2}(1 + 3\omega_x \Omega_x). \tag{3.19}$$

3.2.8 Method for determining z dependence of deceleration parameter

It is necessary to determine how the value of the deceleration parameter changes at increasing redshift values for each of the dark energy models. This being that for these dark energy models there is a transition point between the rate of expansion of the universe decreasing and it beginning to accelerate.

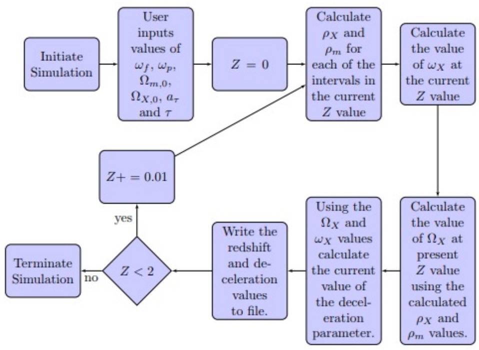

Figure 7: Flowchart used to show the progression through the code to calculate the value of the deceleration parameter at different redshift values for different dark energy and pure matter models.

In order to determine the value of q at different redshift values for these models it was necessary to calculate the value of the dark energy density and density parameter at each of the redshifts using the numerical integration method discussed in section 3.1.3. Through calculating these values it is possible to determine the value of the deceleration parameter at these points using equation 3.19. The general process with which the code accomplishes this is shown in figure 7. As in the case of pure matter universe this value will be constant it provides a useful test of the code to check that it is functioning correctly.

3.3 Investigating modified gravity

3.3.1 H and q in the $\alpha = 1$ modified gravity model.

Here we will determine an expression for the deceleration parameter, q, as a function of a for the $\alpha = 1$ modified gravity model. Here we will include a condensed version of the derivation, the full version can be found in appendix C.2. We start from the modified Friedmann equation:

$$H^2 - \frac{H^\alpha}{r_c^{2-\alpha}} = \frac{8\pi G}{3}\rho_m, \tag{3.20}$$

considering that $\alpha = 1$ and using the present values of H, $H \to H_0$, and density, $\rho_m \to \rho_{m,0}$, we can show that

$$H(a) = H_0 \left[\frac{(1-\Omega_{m,0})^2}{4} - \Omega_{m,0}(\frac{a_0}{a})^3 \right]^{\frac{1}{2}} + \frac{(1-\Omega)H_0}{2}. \tag{3.21}$$

Now, by using the definitions of the deceleration parameter, q, and the Hubble parameter, H, we can derive an expression for q in terms of a, H and dH/da, which we find to be

$$q(z) = -\left(1 + \frac{dH}{da}\frac{a}{H}\right). \tag{3.22}$$

Finally, we can derive q in terms of a using equations 3.21 and 3.22, the result of which will be

$$q = -\left(1 + \frac{(-6(\frac{a_0}{a})^3\Omega_{m,0})}{(1-\Omega_{m,0})^2 + 4\Omega_{m,0}(\frac{a_0}{a})^3 + (1-\Omega_{m,0})\left[(1-\Omega_{m,0}) + 4\Omega_{m,0}(\frac{a_0}{a})^3\right]^{\frac{1}{2}}}\right). \tag{3.23}$$

This is our final expression for q in terms of a for the $\alpha = 1$ modified gravity model.

3.3.2 Present value of acceleration parameter

Now we have a general formula for $q(a)$ we can show that $q < 0$ at present, in this model. We begin by setting the scale factor to its present value. i.e. $a = a_0$. This simplifies our equation down to:

$$q = -\left[1 - \frac{6\,\Omega_{m,0}}{(1-\Omega_{m,0})^2 + 4\,\Omega_{m,0} + (1-\Omega_{m,0})((1-\Omega_{m,0})^2 + 4\,\Omega_{m,0})^{1/2}}\right], \tag{3.24}$$

where $\Omega_{m,0}$ is the density parameter of matter. After expanding out the brackets and cancelling (full derivation included in appendix C.3), we end up with the much simpler expression:

$$q = -\left[1 - \frac{3\,\Omega_{m,0}}{\Omega_{m,0} + 1}\right]. \tag{3.25}$$

We now set $\Omega_{m,0} = 0.308$ (this is the value given in project document) and we find:

$$q = -0.294, \tag{3.26}$$

to 3 significant figures. As we can see $q < 0$ and so we expect to see acceleration at present.

3.3.3 Determining luminosity distance and deceleration values for modified gravity

In order to determine the luminosity distance for the Modified gravity theory it was necessary to calculate the value of the integral of equation 3.27 and use the relation between the physical distance and the luminosity distance.

$$d(z) = \int_{a_z}^{a_0} \frac{c}{a^2\left((H_0)((\frac{1}{4})(1-\Omega_{m,0})^2 + (\Omega_{m,o})(\frac{1}{a})^3)^{\frac{1}{2}} + \frac{(1-\Omega_{m,0})(H_0)}{2}\right)} da. \tag{3.27}$$

In this case, as in the SFQ models, it is not possible to integrate this equation analytically therefore making it necessary to again to use numerical integration techniques. In order to accomplish this the same code and method as previously described in section 3.2.6 may be used with the equation to be integrated altered to this particular case.

As the values of the luminosity distance in this case are now able to be determined, it is possible to compare them with those corresponding to the cosmological constant. Meaning that it can be seen if the two theories may be differentiated from one another.

Furthermore as in the case of the luminosity distance the value of the deceleration parameter at different redshifts is also determined by using a slightly modified version of the code described in section 3.2.8 using equation 3.23. Making it possible to see how the rate of expansion of the universe is altered depending upon the model used.

4 Results and Discussion

4.1 Results for direct evidence measurements

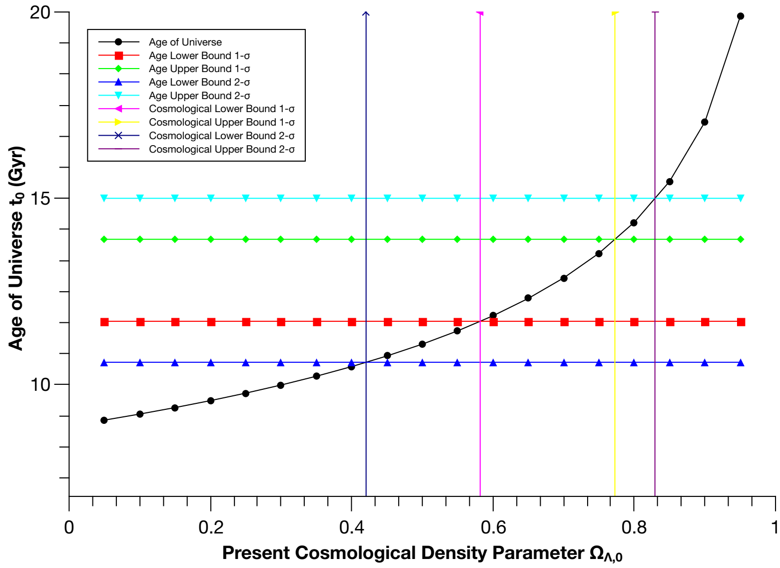

Figure 8: Graph of the age of the universe as a function of the cosmological density parameter. Showing the bounds $1-\sigma$ and $2-\sigma$ on $\Omega_{\Lambda,0}$.

From figure 8 it is clear that the case of $\Omega_{\Lambda,0} = 0$ (pure matter universe) must be ruled out, as the $2-\sigma$[1] lower bound of $\Omega_{\Lambda,0}$ is not zero. As this range of $\Omega_{\Lambda,0}$ is necessary to solve the directly observed age problem and make it consistent with the theoretical age by using the cosmological constant which acts as a component of dark energy.

	$1-\sigma$	$2-\sigma$
Lower Bound	0.5819	0.4204
Upper Bound	0.7726	0.8293

Table 1: $1-\sigma$ and $2-\sigma$ bounds for $\Omega_{\Lambda,0}$ from figure 8.

[1] If the results are within $1-\sigma$ it would mean they are real with a certainty of 68.2%. If results are within $2-\sigma$ they are real with a certainty of 95.4%. So generally the higher the σ values the more confident you can be of your results being real.

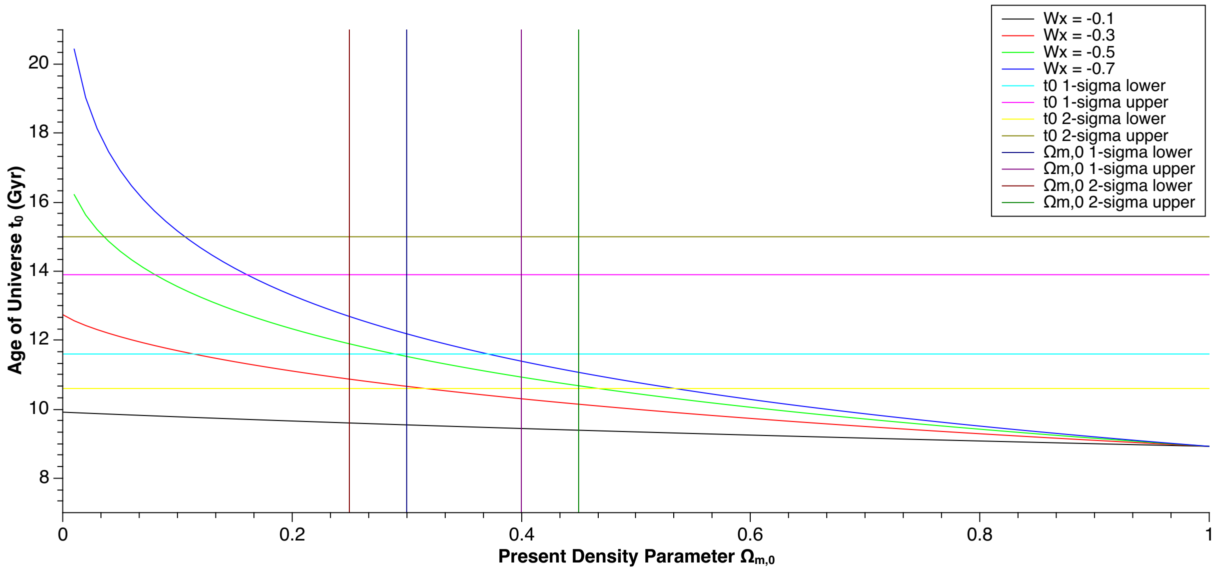

Figure 9: Graph of the age of the universe as a function of the cosmological density parameter. Showing the bounds $1-\sigma$ and $2-\sigma$ on $\Omega_{m,0}$, t_0 and w_x.

From figure 9 we found the values of t_0 for each ω_X when $\Omega_{m,0} = 0.35$. They are presented in table 3.

	$1-\sigma$	$2-\sigma$
Lower Bound	-0.5	-0.25
Upper Bound	-15	approaches a specific curve

Table 2: $1-\sigma$ and $2-\sigma$ bounds for ω_X from figure 9.

ω_X	$t_0(Gyr)$
-0.1	9.4916
-0.3	10.4743
-0.5	11.2117
-0.7	11.7607

Table 3: t_0 values, to 4 decimal places, for ω_X when $\Omega_{m,0} = 0.35$, from figure 9.

4.2 Results for future dark energy experiments

4.2.1 CPL parameterization of EUCLID mission

ω_a	ω_p
0.112	-0.973

Table 4: Values of ω_a and ω_p corresponding to the CPL parameterization for the simulated data.

	$1-\sigma$	$2-\sigma$
ω_a	0.1	0.2
ω_p	0.02	0.04

Table 5: $1-\sigma$ and $2-\sigma$ accuracy's for ω_a and ω_P .

The values of ω_a and ω_p have been stated in table 4. However at $1-\sigma$ and $2-\sigma$ these values differ slightly and enable us to predict if EUCLID will be able to distinguish simulated dark energy from a

	Lower Bound	Upper Bound
ω_a	0.12	0.212
ω_p	-0.993	-0.953

Table 6: $1-\sigma$ bounds for ω_a and ω_P .

	Lower Bound	Upper Bound
ω_a	-0.088	0.312
ω_p	-1.013	-0933

Table 7: $2-\sigma$ bounds for ω_a and ω_P .

cosmological constant. The $1-\sigma$ and $2-\sigma$ accuracy's to which we can measure for ω_a and ω_p are stated in table 5.

Using these we can obtain the upper and lower bounds for ω_a and ω_p. The $1-\sigma$ and $2-\sigma$ bounds will be found in tables 6 and 7 respectively.

So now we can discuss whether EUCLID will be able to distinguish simulated dark energy from a cosmological constant. We can suggest if it is able to do so by using the equation for $\omega_X(a)$ in terms of ω_p and ω_a (Appendix B.2).

If we look at the $1-\sigma$ bounds then we can see that the combinations of ω_a and ω_p will lead to an ω_X value that is not -1,thus making it different to that of the cosmological constant. However at $1-\sigma$ there is only a 68% chance the outcome is right and due to this it is not appropriate to suggest that simulated dark energy will be distinguishable from cosmological constant. Hence, this means at $1-\sigma$ it is not possible to distinguish between the two.

At $2-\sigma$ however, it may be possible to distinguish between the two. This is because using the upper bound values for ω_a and ω_p, results in ω_X being very different to -1. Whereas when we use the lower bounds, we find ω_X is approximately equal to -1. The deciding factor is due to the fact that at $2-\sigma$ there is a 95% likelihood that the values are correct as opposed to a 68% likelihood. Thus $2-\sigma$ provides a more accurate and valid distinction between simulated dark energy and a cosmological constant than $1-\sigma$; but only if the results obtained lie within that $2-\sigma$ range.

Furthermore we can state that ω_X is time dependent (a dependent) for both $1-\sigma$ and $2-\sigma$. For $1-\sigma$ the ω_a values will not be zero at any point, thus ω_X will always be time dependent. For $2-\sigma$ values, ω_X will be time dependent at all points except from when $\omega_a = 0$. At some point ω_a will equal 0 as the range of ω_a is from 0.312 to -0.088. So ω_X is time dependent at the upper and lower limits of ω_a for both $1-\sigma$ and $2-\sigma$.

4.2.2 SFQ model determination of WFIRST

Through using the program previously described in section 3.2.6, it was possible to determine the different luminosity distances at increasing distances for the different models for the Dark energy as well as for the pure matter universe.

Initially it was useful to test the code for the pure cosmological constant and matter cases given that they could be determined analytically and comparing the values given by them with the codes output and seeing if they agree to within an acceptable margin. With the difference between the two being $0.02556Mpc$ and $0.00103Mpc$ for the cosmological constant and pure matter cases respectively at $Z = 2$, given the scales involved these differences can be considered largely negligible for this analysis.

	Redshift (z)	d_L (MPc)
Λ	0.5	2918
	1.32	9570
SFQ 1	0.5	2846
	1.32	9112
SFQ 2	0.5	2910
	1.32	9517
Pure Matter	0.5	2436
	1.32	7051

Table 8: Luminosity distances, to 4 significant figures, of different Dark Energy models

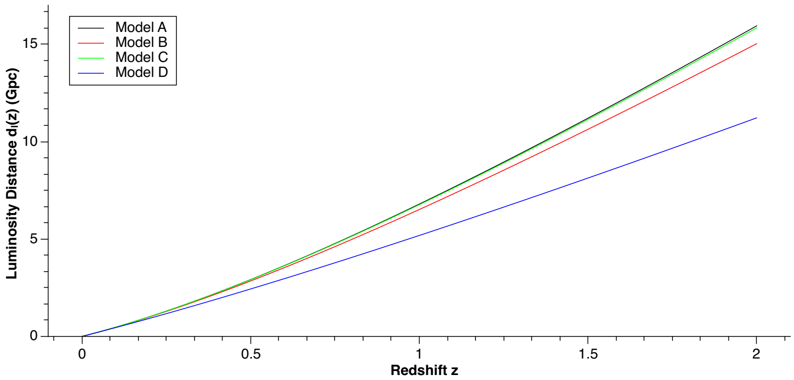

Figure 10: Graph showing the predictions of $d_L(z)$ for the three models of a dark energy universe (A, B and C) and for the model of a pure matter universe (D).

From figure 10 it is apparent that regardless of the dark energy model applied, their luminosity distance is always far greater than that of pure matter, as seen in table 8, with the smallest difference at $Z = 1.32$ still being $2061Mpc$. So, regardless of the dark energy model, it is clearly distinguishable from pure matter.

Furthermore, from figure 11 it can be seen that whilst in the case of pure matter the deceleration parameter remains constant, when dark energy is introduced its value begins to decrease closer to the present time, such that there exists a point when the rate of expansion changes from decreasing to increasing. This point occurring at $Z = 0.6538, 0.4750, 0.6250$ for the cosmological constant, SFQ 1 and SFQ 2 models respectively, as the transition point for SFQ 1 occurs at a significantly smaller redshift than the other models it results in the significantly smaller luminosity distance observed in figure 10.

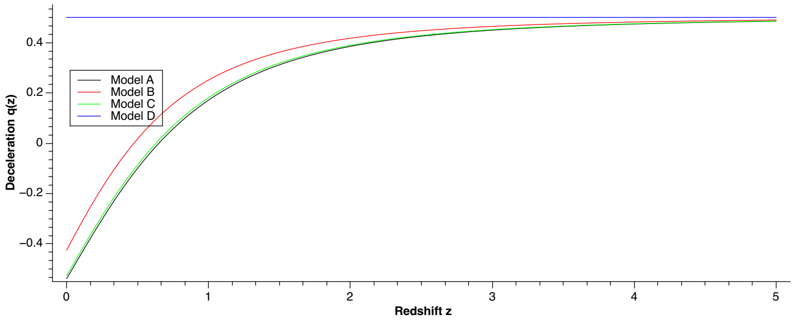

Figure 11: Graph showing redshift deceleration for the three models of a dark energy universe (A, B and C) and for the model of a pure matter universe (D) over the range $0 < z < 5$.

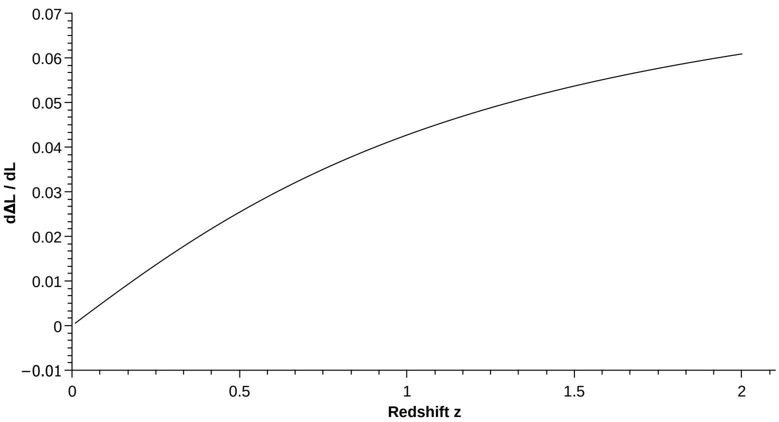

Figure 12: Graph expressing $\frac{\Delta d_L}{d_L}$ as a function of z (for $0 < z < 2$) for the SFQ1 model.

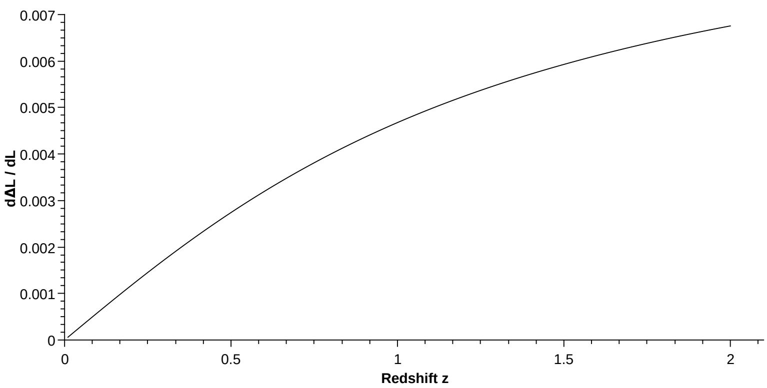

Figure 13: Graph expressing $\frac{\Delta d_L}{d_L}$ as a function of z (for $0 < z < 2$) for the SFQ2 model.

In addition, from figures 12 and 13, in both cases the rate of increase in the fractional difference decreases as the redshift increases. This matches what ought to be expected, as at higher redshift values the universe density and therefore expansion rate will become dominated by matter and then radiation. Thus, this makes the contribution from dark energy negligible, such that regardless of the model their luminosity distance should begin to increase at the same rate. Finally, for WFIRST to be able to distinguish the SFQ models from the cosmological constant their respective fractional differences must be double that of the aggregate precision of WFIRST at the redshift the measurement is made at, with WFIRST having $1-\sigma$ aggregate precision of 0.20% and 0.34% at $Z = 0.50$ and $Z = 1.32$ respectively. So, as the SFQ 1 model has fractional differences of 2.54% at $Z = 0.50$ and 5.03% at $Z = 1.32$%, it may be clearly distinguished from the cosmological constant at both the $1-\sigma$ and $2-\sigma$ ranges. Whilst the SFQ 2 model has fractional differences of 0.274% at $Z = 0.5$ and 0.554% at $Z = 1.32$, this therefore meaning that it can never be distinguished from the cosmological constant as even at $1-\sigma$ at both redshifts there is an overlap of 0.126%.

4.3 An alternative to dark energy

From the data gathered it was also possible to compare the luminosity distances given by the cosmological constant with those produced when modified gravity is applied. This comparison being of particular importance as it may provide a potentially viable alternative to the existence of dark energy, that is capable of explaining the currently observed behaviour.

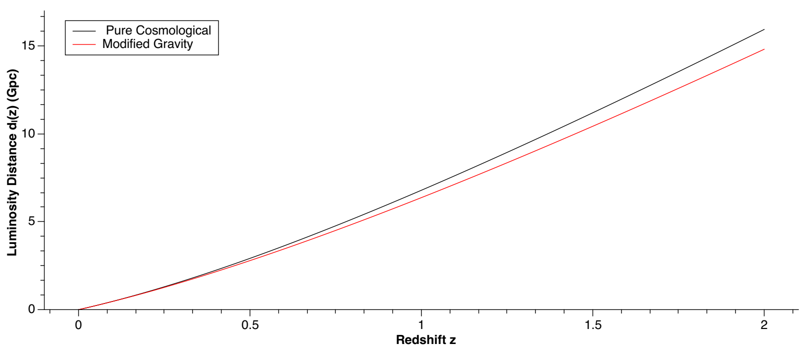

Figure 14: Graph showing the predictions of $d_l(z)$ for the three models of a dark energy universe (A, B and C) and for the model of a pure matter universe (D).

Once again from figure 14 it is clear that use of the modified gravity model will result in larger luminosity distances than for if there existed only pure matter using current gravity models. However it will not be to the same extent as for the cosmological constant. The values of $d_l(z)$ at $z = 0.5$ and $z = 1.32$ were found to be 2.79 GPc and 8.929 GPc respectively.

This being highlighted from figure 15 where the transition point for the modified gravity model

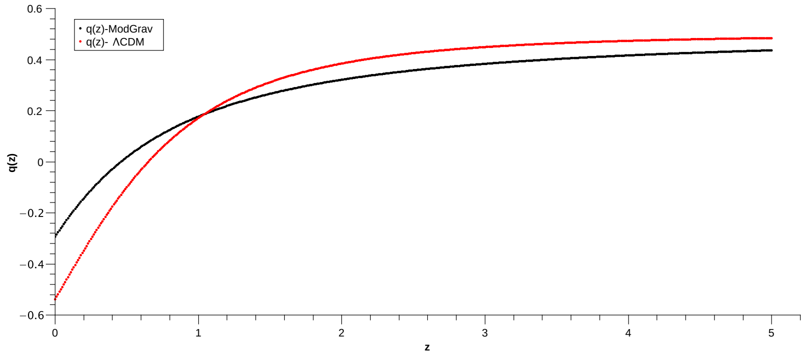

Figure 15: Graph depicting deceleration parameter, q(z), as a function of redshift, z, for the Modified Gravity and ΛCDM models of the universe, for redshift values $0 < z < 5$.

occurring at $Z = 0.4586$ whilst for the cosmological constant it occurs at $Z = 0.6538$. So as it occurs at a lower redshift for modified gravity the universe will have been undergoing accelerated expansion for a shorter period of time than in the case of the cosmological constant. This being the same as what occurs for the SFQ models.

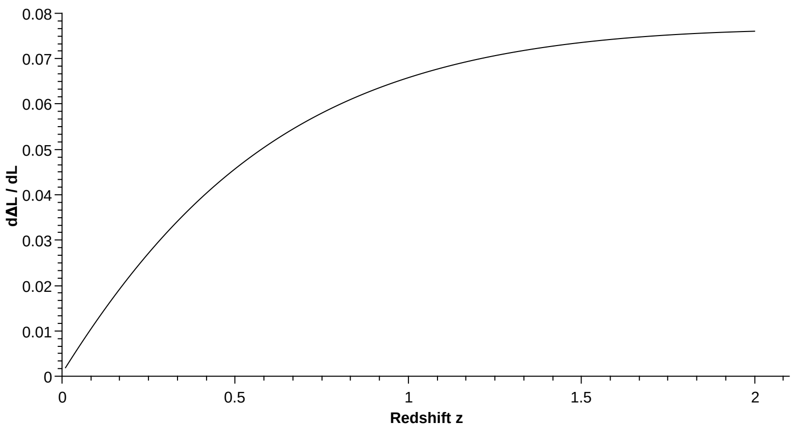

Figure 16: Graph expressing $\frac{\Delta d_L}{d_L}$ as a function of z (for $0 < z < 2$) for the Modified Gravity Model.

Furthermore from figure 16 it can be seen that the rate of increase in the fractional difference decreases as the redshift increase, just as in the case of the SFQ models meaning that the expansion will still go back to being matter and radiation dominated when using the standard Friedmann equation. Once again for WFIRST to distinguish the modified gravity model from the cosmological constant its fractional difference must be double that of the aggregate precision of WFIRST at the redshift the result is taken at. As WFIRST has aggregate precision's of 0.20% and 0.34% at $1-\sigma$ for redshifts $Z = 0.5$ and $Z = 1.32$ respectively. As the modified gravity has fractional differences of 4.57% and 7.16% at these redshifts. It is clearly distinguishable from the cosmological constant at both redshifts in both the $1-\sigma$ and $2-\sigma$ ranges.

5 Conclusion

Initially in our investigations into dark energy, we were able to determine that for the observed range for the age of the universe to be allowed there must exist some form of dark energy and just regular matter. Such that in the case of a cosmological constant, $\Omega_{m,0}$ had a $2-\sigma$ range of 0.4204 to 0.8239, so there must be another substance present. When we considered that dark energy may not be constant with baratropic parameter of $\omega_X = -1$ and that its value may vary, it was found that for the $1-\sigma$ range it could have a value between -15 and -0.5. Whereas at $2-\sigma$ there is a lower limit of -0.25 and no upper limit as it is impossible to reach one. This therefore shows that it is possible for ω_X, at present, to take a range of values, whilst still having the age of the universe within the expected range, thus allowing for other dark energy models to exist.

One of these models that was investigated was the CPL parameterisation and how it may be identified by the EUCLID mission. In this case the values of ω_a and ω_p were determined to be 0.112 and -0.973 respectively, for the given set of simulated data. If the real values are found to be the same or similar to these, we determined that it would be possible for the EUCLID mission to distinguish these values at the $1-\sigma$ range from the cosmological constant, however at the $2-\sigma$ range they become too similar to allow them to be distinguished. Therefore whilst it may be possible to determine the values in this case, as the $1-\sigma$ range only has 68% probability of being correct, it would not be possible to be certain that this model is correct.

Furthermore, we also determined whether the WFIRST mission could distinguish the SFQ 1 and 2 models as well as the modified gravity model from the cosmological constant. This determination being made at redshifts $z = 0.5$ and $z = 1.32$. For both the SFQ1 and modified gravity, they can be easily distinguished at both the $1-\sigma$ and $2-\sigma$ ranges from the cosmological constant at both redshifts, given that they have fractional differences of 2.54% and 5.03% and 4.57% and 7.16% respectively. However, in the case of the SFQ 2 model it cannot be distinguished from the cosmological constant at either redshift value given that in both cases at $1-\sigma$ there is an overlap of 0.126%. So, if either the SFQ 1 or cosmological constant models are correct it will not be possible to determine which of them it is.

This study may be further improved by both improving the code that was used such that it may possess a more modular design, making it more versatile and undertake a larger range of tasks. Furthermore, it may be useful to examine the fractional difference between the SFQ models and the modified gravity theory to determine whether they might be confused for one another by the WFIRST mission. Additionally, it may be prudent to test a wider range of dark energy theories and alternatives to it so that there is a wider base to draw information from as well as attempt to improve the precision of WFIRST so that it might be able to distinguish the SFQ 2 model from the cosmological constant.

Appendices

A Direct evidence for dark energy

A.1 Derivation of t_0 as a function of Ω_Λ^0

Starting with the Friedmann equation for the case of a flat universe we will derive the equation for the age of the universe at present time.

$$H^2 = \left(\frac{\dot{a}}{a}\right)^2 = \frac{8\pi G\rho_c}{3}, \tag{A.1}$$

Integrating the LHS with respect to the scale factor and the RHS with respect to time

$$\int_0^a \frac{1}{a\rho_c^{\frac{1}{2}}} da = \int_0^t \sqrt{\frac{8\pi G}{3}} dt, \tag{A.2}$$

and then substitute in $\rho_c = \rho_m + \rho_\Lambda$.

$$\int_0^a \frac{1}{a\sqrt{\rho_m + \rho_\Lambda}} da = \int_0^t \sqrt{\frac{8\pi G}{3}} dt, \tag{A.3}$$

We then know that $\rho_m = (\frac{a_0}{a})^3 \rho_{m,0}$ which can be derived from the continuity equation. If we just consider the derivation for the LHS of the equation first,

$$\int_0^a \frac{a^{\frac{1}{2}}}{\sqrt{a_0^3\rho_{m,0} + a^3\rho_\Lambda}} da, \tag{A.4}$$

and let $\beta = a_0^3\rho_{m,0}$ and $\alpha = \rho_\Lambda$. We get,

$$\frac{1}{\sqrt{\beta}} \int_0^a a^{\frac{1}{2}} \frac{1}{\sqrt{\frac{a^3\alpha}{\beta} + 1}} da, \tag{A.5}$$

and again if we let $k = \frac{\alpha}{\beta}$ and substituting $s = a^{\frac{3}{2}} k^{\frac{1}{2}}$ so $da = \frac{2}{3} a^{-\frac{1}{2}} k^{-\frac{1}{2}}$ we get,

$$\frac{1}{\sqrt{\beta}} \frac{2\sqrt{\beta}}{3\sqrt{\alpha}} \int_0^s \frac{1}{\sqrt{s^2+1}} ds, \tag{A.6}$$

which then can be simplified to,

$$\frac{2}{3\sqrt{\alpha}}\int_0^{a^{\frac{2}{3}}\sqrt{k}}\frac{1}{\sqrt{s^2+1}}ds. \tag{A.7}$$

Integrating this and substituting in the upper and lower limits

$$\frac{2}{3\sqrt{\alpha}}\sinh^{-1}(a^{\frac{3}{2}}\sqrt{k}), \tag{A.8}$$

but we know that $\sinh^{-1}(x) = \ln[x+\sqrt{x^2+1}]$, so using this and also $k = \frac{\alpha}{\beta}$ where $\beta = a_0^3\rho_{m,0}$ and $\alpha = \rho_\Lambda$

$$\frac{2}{3\sqrt{\rho_\Lambda}}\ln\left[\sqrt{\frac{\rho_\Lambda a^3}{\rho_{m,0}a_0^3}}+\sqrt{\frac{\rho_\Lambda a^3}{\rho_{m,0}a_0^3}+1}\right], \tag{A.9}$$

We know that $\rho_m = \frac{a_0^3}{a^3}\rho_{m,0}$, stated previously, so substituting this in we get,

$$\frac{2}{3\sqrt{\rho_\Lambda}}\ln\left[\sqrt{\frac{\rho_\Lambda}{\rho_m}}+\sqrt{\frac{\rho_\Lambda}{\rho_m}+1}\right], \tag{A.10}$$

but we know $\rho_\Omega = \Omega_\Lambda\rho_0$ and $\rho_m = \Omega_m\rho_0$ from the density parameter equation. Substituting these in we get,

$$\frac{2\rho_0^{-\frac{1}{2}}}{3\sqrt{\Omega_\Lambda}}\ln\left[\sqrt{\frac{\Omega_\Lambda}{\Omega_m}}+\sqrt{\frac{\Omega_\Lambda+\Omega_m}{\Omega_m}}\right], \tag{A.11}$$

and we want this equation in terms of present parameters so, $\Omega_\Lambda \to \Omega_{\Lambda,0}$ and $\Omega_m \to \Omega_{m,0}$

$$\frac{2\rho_0^{-\frac{1}{2}}}{3\sqrt{\Omega_{\Lambda,0}}}\ln\left[\sqrt{\frac{\Omega_{\Lambda,0}}{\Omega_{m,0}}}+\sqrt{\frac{\Omega_{\Lambda,0}+\Omega_{m,0}}{\Omega_{m,0}}}\right], \tag{A.12}$$

so using $\Omega_{m,0}+\Omega_{\Lambda,0} = 1 \to \Omega_{m,0} = 1-\Omega_{\Lambda,0}$ for a flat universe and re-arranging for the final part of the LHS we get

$$\frac{2\rho_0^{-\frac{1}{2}}}{3\sqrt{\Omega_{\Lambda,0}}}\ln\left[\frac{1+\sqrt{\Omega_{\Lambda,0}}}{\sqrt{1-\Omega\Lambda,0}}\right], \tag{A.13}$$

Now considering the RHS of equation 2. We can re-arrange equation 1 for present time to get

$$H_0\rho_0^{-\frac{1}{2}} = \sqrt{\frac{8\pi G}{3}}, \tag{A.14}$$

and substituting this into the integral where the upper limit $t \to t_0$

$$\int_0^{t_0} H_0 \rho_0^{-\frac{1}{2}} dt, \tag{A.15}$$

Solving this integral and plugging in the upper and lower limits we get

$$H_0 \rho_0^{\frac{-1}{2}} t_0, \tag{A.16}$$

Now setting the LHS and RHS we found,

$$\frac{2\rho_0^{\frac{-1}{2}}}{3\sqrt{\Omega_{\Lambda,0}}} \ln\left[\frac{1+\sqrt{\Omega_{\Lambda,0}}}{\sqrt{1-\Omega\Lambda,0}}\right] = H_0 \rho_0^{\frac{-1}{2}} t_0, \tag{A.17}$$

Finally, cancelling down and re-arranging for t_0 we get,

$$t_0 = \frac{2}{3}\frac{H_0^{-1}}{\sqrt{\Omega_{\Lambda,0}}} \ln\left[\frac{1+\sqrt{\Omega_{\Lambda,0}}}{\sqrt{1-\Omega_{\Lambda,0}}}\right], \tag{A.18}$$

This is the final result for the age of the universe for present time.

A.2 Derivation of t_0 as a function of Ω_m^0 for different ω_X

Here we will obtain the expression for t_0 as a function of $\Omega_{m,0}$ for different ω_X. This expression contains an integral that will need to be numerically integrated, and we will first derive this integral. We will start by using equation A.3 for the case where ρ_Λ is replaced by $\rho_X(a)$, where the a dependence of $\rho_X(a)$ is determined by ω_X.

So the density of dark energy will now vary with scale factor according to

$$\rho_\Lambda = \rho_X(a) = \rho_{0,X}\left(\frac{a_0}{a}\right)^{3(1+\omega_X)}, \tag{A.19}$$

Substituting this into the LHS of equation A.3 will give

$$I = \int_0^a \frac{1}{a\left[\rho_m + \rho_{0,X}\left(\frac{a_0}{a}\right)^{3(1+\omega_X)}\right]^{\frac{1}{2}}} da, \tag{A.20}$$

We can replace ρ_m with

$$\rho_m = \left(\frac{a_0}{a}\right)^3 \rho_{m,0}, \tag{A.21}$$

Which will give

$$I = \int_0^a \frac{1}{a\left[\left(\frac{a_0}{a}\right)^3 \rho_{m,0} + \rho_{0,X}\left(\frac{a_0}{a}\right)^{3(1+\omega_X)}\right]^{\frac{1}{2}}} da, \tag{A.22}$$

Where $\rho_{m,0}$ can be expressed in terms of $\Omega_{m,0}$

$$\Omega_{m,0} = \frac{\rho_{m,0}}{\rho_c}, \tag{A.23}$$

And $\rho_{m,0}$, ρ_c are the critical density and current matter density respectively.

We now have the integral in a form we can numerically integrate, hence we can focus on the RHS of equation A.3. From using the equation for critical density we can say

$$\rho_c = \rho_0 = \frac{3H^2}{8\pi G}, \tag{A.24}$$

Rearranging this will give

$$\frac{H^2}{\rho_0} = \frac{8\pi G}{3}, \tag{A.25}$$

This can be substituted into the RHS of A.3 to give

$$I = t_0\left(\frac{H^2}{\rho_0}\right)^{\frac{1}{2}}, \tag{A.26}$$

We want this equation in terms of the present parameters, so $H \to H_0$,

$$I = t_0\frac{H_0}{\rho_0{}^{\frac{1}{2}}}, \tag{A.27}$$

Rearrange to find t_0

$$t_0 = I\frac{\rho_0{}^{\frac{1}{2}}}{H_0}, \tag{A.28}$$

Hence we have derived the expression for t_0 as a function of $\Omega_{m,0}$ for different ω_X. This expression for t_0 will have an upper bound as $\omega_X \to -\infty$. So as ω_X becomes negatively large the curve is shifted by an incredibly small amount. This is because the $\rho_X(a)$ becomes very close to zero and so we are left with a matter dominated universe. This can be shown as follows, firstly we set $a_0 = 1$ in equation A.22.

Next, as $\omega_X \to -\infty$, then

$$\rho_{0,X}\left(\frac{a_0}{a}\right)^{3(1+\omega_X)} \to 0, \tag{A.29}$$

Which will lead to give us

$$I = \int_0^1 \frac{1}{a\left[\left(\frac{1}{a}\right)^3 \rho_{m,0}\right]^{\frac{1}{2}}} da, \tag{A.30}$$

simplifying this down we get,

$$I = \rho_{m,0}{}^{-\frac{1}{2}} \int_0^1 a^{\frac{1}{2}} da, \tag{A.31}$$

$$I = \frac{2}{3}\rho_{m,0}{}^{-\frac{1}{2}}, \tag{A.32}$$

Substituting this is into the expression for t_0 will give us

$$t_0 = \frac{2}{3}\frac{\rho_c{}^{\frac{1}{2}}}{\rho_{m,0}{}^{\frac{1}{2}}}\frac{1}{H_0}, \tag{A.33}$$

We can rewrite this using equation A.23

$$t_0 = \frac{2}{3}\frac{1}{\Omega_{m,0}^{\frac{1}{2}} H_0}, \tag{A.34}$$

Thus we have derived the upper bound on t_0 as a function of $\Omega_{m,0}$ when $\omega_X \to -\infty$.

A.3 Code to Determine the Value of t_0 for different ω_x values

```
from math import pi
from math import exp
from math import inf

H_0 = float((73.2E3)*(3.086E22)**(-1))
G = float(6.67E-11)
```

```
w_x = float(input("What is wx value" + "\n"))
N = int(1000)

results = open("Age_of_Universe.txt","w")

def p_x_o_calc(Om_X_o):
    y = 3*((H_0)**2)
    i = 8 * pi * G
    u = y/i
    p_x_o = Om_X_o * u
    return p_x_o

def p_m_o_calc(Om_M_o):
    y = 3*((H_0)**2)
    i = 8 * pi * G
    u = y/i
    p_m_o = Om_M_o * u
    return p_m_o

def p_m_calc(p_m_o,a_z):
    y = 1/a_z
    i = y**3
    p_m = i * p_m_o
    return p_m

def p_x_calc(p_x_o,a,w):
    y = 1/(a)
    i = y**(3*(1+w))
    p_x = i * p_x_o
    return p_x

def part_func(a_z,p_x,p_m):
    y = (p_x + p_m)**(-1/2)
    z = (1/(a_z))*y
    return z

for p in range(0,101):
    ohm_m_o = float(p*0.01)
```

```
    ohm_x_o = 1 - ohm_m_o

    p_m_o = p_m_o_calc(ohm_m_o)
    p_x_o = p_x_o_calc(ohm_x_o)

    a_z = float(1E-90)

    p_x = p_x_calc(p_x_o,a_z,w_x)
    p_m = p_m_calc(p_m_o, a_z)

    h = (1-a_z)/float(N)
    s = 0.5*((part_func(a_z,p_x,p_m)) + (part_func(1,p_x_o,p_m_o)))

    for i in range(1,N,1):
        r = a_z + i*h
        p_x = p_x_calc(p_x_o,r,w_x)
        p_m = p_m_calc(p_m_o,r)
        s = s + part_func(r,p_x,p_m)

    I = s*h

    H = (3/(8*pi*G))**(1/2)

    t = (I*H)/(3.15E16)

    results.write(str(ohm_m_o) + " , " + str(t) + "\n")

results.close()
```

B DETERMINING THE NATURE OF DARK ENERGY

B.1 Preliminary Calculations

It was first necessary to be able to determine the physical distance as a function of the redshift to be used in future calculations. In order to do this must first consider the relations,

$$dr = c\,dt \quad \text{and} \quad dr = a(t)\,dX. \tag{B.1}$$

Which may be altered such that,

$$cdt = a(t)dX \quad \text{so} \quad dX = \frac{c}{a(t)}dt, \tag{B.2}$$

finally producing the relationship with the comoving distance as being,

$$X = \int_{t_i}^{t_0} \frac{c}{a(t)}dt \quad \text{and as} \quad d(z) = a(t_0)dX, \tag{B.3}$$

it can be determined that,

$$d(z) = a(t_0)\int_{t_i}^{t_0} \frac{c}{a(t)}dt. \tag{B.4}$$

In order to alter equation B.4 such that it is only a function of the scale factor and therefore redshift must make use of the relationship,

$$H = \frac{1}{a}\frac{da}{dt}, \tag{B.5}$$

to produce the desired equation of

$$d(z) = a_0\int_{a(z)}^{a_0} \frac{c}{a^2 H(a)}da. \tag{B.6}$$

In order to determine the relationship for the $H(a)$ term it was necessary to use the general form of equation A.1 to produce the relationship,

$$H = \sqrt{\frac{8\pi G}{3}}(\rho_m + \rho_x)^{1/2}. \tag{B.7}$$

As the value of the barotropic parameter ω_X will vary the relationship between ρ_X and the scale factor can be found to be,

$$\rho_x = e^{-\int_{a_0}^{a(z)} \frac{3(1+\omega_x(a))}{a}da}\rho_{x,0}. \tag{B.8}$$

As the equation for ρ_m is still that of equation A.21 these may be substituted into equation B.7 and in turn equation B.6 to produce the final equation,

$$d(z) = a_0 \int_{a(z)}^{a_0} \frac{c}{a^2 \sqrt{\frac{8\pi G}{3}} \left(\left(\frac{a_0}{a}\right)^3 \rho_{m,0} + e^{-\int_{a_0}^{a(z)} \frac{3(1+\omega_X(a))}{a} da} \rho_{x,0} \right)^{1/2}} da \tag{B.9}$$

B.2 Derivation of the CPL Parameterization for a flat universe for d(z)

For this derivation we need to rearrange equation B.8, and express as:

$$\ln \frac{\rho_X(a)}{\rho_{X,0}} = -\int_{a_0}^{a} \frac{3(1+\omega_X(a))}{a} da, \tag{B.10}$$

Set $a_p = a_0$, thus:

$$\omega_X(a) \equiv \frac{\rho_X}{\rho_{X,0}} = \omega_p + \left(1 - \frac{a}{a_0}\right)\omega_a, \tag{B.11}$$

substituting equation B.11 into RHS of equation B.10 we get the integral to be:

$$= -\int_{a_0}^{a} \frac{3(1+\omega_p + (1-\frac{a}{a_0})\omega_a)}{a} da, \tag{B.12}$$

expanding and collecting terms gives:

$$= -\int_{a_0}^{a} \frac{3+3\omega_p+3\omega_a}{a} - \frac{3\omega_a}{a_0} da, \tag{B.13}$$

remove negative sign by flipping limits and integrate:

$$= \int_{a}^{a_0} \frac{3(1+\omega_p+\omega_a)}{a} - \frac{3\omega_a}{a_0} da, \tag{B.14}$$

$$= 3(1+\omega_p+\omega_a) \ln a \Big|_a^{a_0} - \frac{3\omega_a a}{a_0}\Big|_a^{a_0}, \tag{B.15}$$

gives...

$$= 3(1+\omega_p+\omega_a) \ln \frac{a_0}{a} - \left(3\omega_a - \frac{3\omega_a a}{a_0}\right), \tag{B.16}$$

equating with LHS and expressing as follows:

$$\ln\frac{\rho_X(a)}{\rho_{X,0}} = \ln\frac{a_0}{a}^{3(1+\omega_p+\omega_a)} - 3\omega_a\Big(1-\frac{a}{a_0}\Big), \tag{B.17}$$

the next step is to take exponential on both sides, which leaves:

$$\frac{\rho_X(a)}{\rho_{X,0}} = \frac{a_0}{a}^{3(1+\omega_p+\omega_a)} e^{-3\omega_a(1-\frac{a}{a_0})}, \tag{B.18}$$

or..

$$\rho_X(a) = \rho_{X,0}\Big(\frac{a_0}{a}^{3(1+\omega_p+\omega_a)} e^{-3\omega_a(1-\frac{a}{a_0})}\Big). \tag{B.19}$$

Now using equation B.6 from the Preliminary calculations:

$$d(z) = a_0\int_{a(z)}^{a_0}\frac{c}{a^2 H(a)}da \tag{B.20}$$

where:

$$H(a) = \sqrt{\frac{8\pi G}{3}}\rho^{\frac{1}{2}} \qquad \text{and} \qquad \rho = \rho_m + \rho_X(a) \tag{B.21}$$

also incorporating the fact that:

$$\rho_c = \frac{3H^2}{8\pi G} \qquad \rightarrow \qquad \frac{H_0}{\rho_{c,0}^{\frac{1}{2}}} = \sqrt{\frac{8\pi G}{3}} \tag{B.22}$$

Thus subbing the above into equation B.20 will produce:

$$d(z) = a_0\int_{a(z)}^{a_0}\frac{c}{a^2\frac{H_0}{\sqrt{\rho_{c,0}}}(\rho_m+\rho_X(a))^{\frac{1}{2}}}da \tag{B.23}$$

and then for the next step, sub equation B.19 into the above and express as:

$$d(z) = a_0\int_{a(z)}^{a_0}\frac{c}{a^2\frac{H_0}{\sqrt{\rho_{c,0}}}\Big[\rho_m+\rho_{X,0}(\frac{a_0}{a})^3\Big((\frac{a_0}{a})^{3(\omega_p+\omega_a)}e^{-3\omega_a(1-\frac{a}{a_0})}\Big)\Big]^{\frac{1}{2}}}da \tag{B.24}$$

and as:

$$\rho_m = \rho_{m,0}(\frac{a_0}{a})^{3(1+\omega_m)} \quad , \quad \omega_m = 0 \quad , \quad \rho_m = \rho_{m,0}(\frac{a_0}{a})^3 \tag{B.25}$$

then,

$$d(z) = a_0 \int_{a(z)}^{a_0} \frac{c}{a^2 \frac{H_0}{\sqrt{\rho_{c,0}}} (\frac{a_0}{a})^{\frac{3}{2}} \left[\rho_{m,0} + \rho_{X,0}\left((\frac{a_0}{a})^{3(\omega_p+\omega_a)} e^{-3\omega_a(1-\frac{a}{a_0})}\right)\right]^{\frac{1}{2}}} da \tag{B.26}$$

will cancel down to:

$$d(z) = \frac{c}{H_0 a_0^{\frac{1}{2}}} \int_{a(z)}^{a_0} \frac{da}{a^{\frac{1}{2}} \left[\frac{\rho_{m,0}}{\rho_{c,0}} + \frac{\rho_{X,0}}{\rho_{c,0}}\left((\frac{a_0}{a})^{3(\omega_p+\omega_a)} e^{-3\omega_a(1-\frac{a}{a_0})}\right)\right]^{\frac{1}{2}}} \tag{B.27}$$

and finally, using:

$$\frac{\rho_{i,0}}{\rho_{c,0}} = \Omega_{i,0} \tag{B.28}$$

the formula for the CPL Parameterization for a flat universe for d(z) can be expressed in its desired form of:

$$d(z) = \frac{c}{H_0 a_0^{\frac{1}{2}}} \int_{a(z)}^{a_0} \frac{da}{a^{\frac{1}{2}} \left[\Omega_{m,0} + \Omega_{X,0}\left((\frac{a_0}{a})^{3(\omega_p+\omega_a)} e^{-3\omega_a(1-\frac{a}{a_0})}\right)\right]^{\frac{1}{2}}} \tag{B.29}$$

B.3 Code to Determine values of ω_a and ω_p

```
from math import pi
from math import exp
from math import inf
from math import log
from math import floor
from math import log10
```

```
H_0 = float(67.81E3)
G = float(6.67408E-11)
N = int(10000)
l_BAO = float(147.60)
Ohm_M = float(0.308)
Ohm_X = float(0.692)
c = float(2.998E8)

z_1 = float(input("Value of  first redshift \n"))
Theta_1 = float(input("Value of first theta \n"))

z_2 = float(input("Value of second redshift \n"))
Theta_2 = float(input("Value of second theta \n"))

results = open("W_p_W_A_finder.txt","w")

def round_sigfigs(num, sig_figs):
    if num != 0:
        return round(num, -int(floor(log10(abs(num))) - (sig_figs - 1)))

def d_Z_calc(Theta):
    y = (l_BAO)/(Theta)
    return y

def d_z_int(w_p,w_a,a):
    y = a**(-0.5)*(Ohm_M + Ohm_X*((1/a)**(3*(w_p + w_a)))*exp(3*w_a*(a - 1)))**(-0.5)
    return y

d_z_1_comp = round_sigfigs(d_Z_calc(Theta_1),6)
d_z_2_comp = round_sigfigs(d_Z_calc(Theta_2),6)


for r in range(-9800,-9699,1):
    w_p = float(r) * 0.0001
    for t in range(1100,1201,1):
        w_a = float(t) * 0.0001
        a_z_1 = 1/(1+z_1)
```

```
    a_z_2 = 1/(1+z_2)
    h_1 = (1-a_z_1)/float(N)
    h_2 = (1-a_z_2)/float(N)

    s_1 = 0.5*(d_z_int(w_p,w_a,a_z_1) + d_z_int(w_p,w_a,1))
    s_2 = 0.5*(d_z_int(w_p,w_a,a_z_2) + d_z_int(w_p,w_a,1))

    for i in range(1,N,1):
        r_1 = a_z_1 + i*h_1
        r_2 = a_z_2 + i*h_2

        s_1 = s_1 + d_z_int(w_p,w_a,r_1)
        s_2 = s_2 + d_z_int(w_p,w_a,r_2)

    d_z_1_int = s_1 * h_1
    d_z_2_int = s_2 * h_2

    d_z_1 = round_sigfigs(d_z_1_int * (c) * (1/H_0),6)

    d_z_2 = round_sigfigs(d_z_2_int * c * (1/H_0),6)

    results.write(str(d_z_1_comp) + " , " + str(d_z_1) + " , "
    + str(d_z_2_comp) + " , " + str(d_z_2) + "\n")

    if d_z_1 == d_z_1_comp and d_z_2 == d_z_2_comp:
        print(str(w_a) + " , " + str(w_p))
```

B.4 Code used to Calculate the value of the Luminosity Distance for Different Dark Energy Models

```
from math import pi
from math import exp
from math import inf

H_0 = float(67.81E3)
G = float(6.67E-11)
N = int(1000)

w_p = float(input('enter the value of w_past \n '))
```

```
w_f = float(input('enter the value of w_f \n '))
T = float(input('enter the value of T \n '))
a_T = float(input('enter the value of a_T \n '))
Omega_X0 = float(input('enter the value of Omega_X0 \n '))
Omega_m0 = float(input('enter the value of Omega_m0 \n '))

results = open("calculated_values.txt","w")

results.write("Redshift" + " , " + "Luminosity Distance" + "/n")

def p_x_o_calc(Om_X_o):
    y = 3*((H_0)**2)
    i = 8 * pi * G
    u = y/i
    p_x_o = Om_X_o * u
    return p_x_o

def p_m_o_calc(Om_M_o):
    y = 3*((H_0)**2)
    i = 8 * pi * G
    u = y/i
    p_m_o = Om_M_o * u
    return p_m_o

def p_m_calc(p_m_o,a_z):
    y = 1/a_z
    i = y**3
    p_m = i * p_m_o
    return p_m

def w_x_calc(a_z):
    w_x = float(w_f + ((w_p - w_f) / (1 + (a_z / a_T)**(1/(T)))))
    return w_x

def d_z_int1(a_z):
    return ((3E8)/((a_z)**2))

def p_x_integrate_func(a_z):
```

```
    return ((3*(1 + w_x_calc(a_z)))/(a_z))

def p_x_calc(y,p_x_o):
    i = exp(-y) * (p_x_o)

def H_calc(p_x,p_m):
    y = ((8 * pi * G)/3)**(1/2)
    i = y*(p_x + p_m)**(1/2)

for x in range(0,201):

    z = float(x*0.01)
    a_z = 1/(1+z)

    p_x_o = p_x_o_calc(Omega_X0)
    p_m_o = p_m_o_calc(Omega_m0)

    p_m_a_t = p_m_calc(p_m_o,a_z)

    h_x = (a_z - 1)/float(N)
    s_x = 0.5*(p_x_integrate_func(1) + p_x_integrate_func(a_z))
    for i in range(1,N,1):
        r = 1 + i*h_x
        s_x = s_x + p_x_integrate_func(r)

    s_x_comp = s_x * h_x
    p_x_a_t = p_x_calc(s_x_comp,p_x_o)

    h = (1-a_z)/float(N)
    H = H_calc(p_x_a_t,p_m_a_t)
    s = 0.5*(((d_z_int1(a_z))/(H)) + ((d_z_int1(1))/(H_0)))

    for i in range(1,N,1):
        r = a_z + i*h

        p_m_a_t = p_m_calc(p_m_o,r)
        y = d_z_int1(r)
```

```
        h_x = (r - 1)/float(N)
        s_x = 0.5*(p_x_integrate_func(1) + p_x_integrate_func(r))

        for j in range(1,N,1):
            u = 1 + j*h_x
            s_x = s_x + p_x_integrate_func(u)

        s_x_comp = s_x * h_x
        p_x_a_t = p_x_calc(s_x_comp,p_x_o)

        H = H_calc(p_x_a_t,p_m_a_t)
        s = s + (y/(H))

    d_z = s*h

    d_L = (1+z)*(d_z)
    results.write(str(z) + " , " + str(d_L) + "\n")
results.close()
```

B.5 Code Used to Calculate Value of Deceleration Parameter

```
from math import pi
from math import exp
from math import inf

H_0 = float(67.81E3)
G = float(6.67E-11)
N = int(10000)

w_p = float(input('enter the value of w_past \n '))
w_f = float(input('enter the value of w_f \n '))
T = float(input('enter the value of T \n '))
a_T = float(input('enter the value of a_T \n '))
Omega_X0 = float(input('enter the value of Omega_X0 \n '))
Omega_m0 = float(input('enter the value of Omega_m0 \n '))

results = open("calculated_values.txt","w")
```

```
results.write("Redshift" + " , " + "Deceleration Value" + "\n")

def p_x_o_calc(Om_X_o):
    y = 3*((H_0)**2)
    i = 8 * pi * G
    u = y/i
    p_x_o = Om_X_o * u
    return p_x_o

def p_m_o_calc(Om_M_o):
    y = 3*((H_0)**2)
    i = 8 * pi * G
    u = y/i
    p_m_o = Om_M_o * u
    return p_m_o

def p_m_calc(p_m_o,a_z):
    y = 1/a_z
    i = y**3
    p_m = i * p_m_o
    return p_m

def w_x_calc(a_z):
    w_x = float(w_f + ((w_p - w_f) / (1 + (a_z / a_T)**(1/(T)))))
    return w_x

def d_z_int1(a_z):
    return ((3E8)/((a_z)**2))

def p_x_integrate_func(a_z):
    return ((3*(1 + w_x_calc(a_z)))/(a_z))

def p_x_calc(y,p_x_o):
    i = exp(-y) * (p_x_o)
    return i

def H_calc(p_x,p_m):
    y = ((8 * pi * G)/3)**(1/2)
```

```
    i = y*(p_x + p_m)**(1/2)
    return i

for x in range(0,501):
    z = float(x*0.01)
    a_z = 1/(1+z)
    p_x_o = p_x_o_calc(Omega_X0)
    p_m_o = p_m_o_calc(Omega_m0)
    p_m_a_t = p_m_calc(p_m_o, a_z)

    h_x = (a_z - 1)/float(N)
    s_x = 0.5*(p_x_integrate_func(1) + p_x_integrate_func(a_z))
    for i in range(1,N,1):
        r = 1 + i*h_x
        s_x = s_x + p_x_integrate_func(r)

    s_x_comp = s_x * h_x
    p_x_a_t = p_x_calc(s_x_comp, p_x_o)

    p_c = p_m_a_t + p_x_a_t
    ohm_x = (p_x_a_t)/(p_c)
    w_x = w_x_calc(a_z)
    q = 0.5*(1 + 3*(w_x)*(ohm_x))

    results.write(str(z) + " , " + str(q) + "\n")

results.close()
```

C AN ALTERNATIVE TO DARK ENERGY

C.1 Modified Gravity Luminosity Distance Code

```
from math import pi

H_0 = float(67.81E3)
G = float(6.67E-11)
c = float(2.998E8)
N = int(10000)
```

```
Ohm_m_0 = float(input("What is the value of Ohm_m_0 \n"))

results = open("ModifiedGravityValues.txt","w")

results.write("Redshift ,  Luminosity Distance" + "\n")

def H_calc(a):
    H_1 = (H_0)*((1/4)*(1 - Ohm_m_0)**(2) + (Ohm_m_0)*(1/a)**(3))**(1/2)
    H_2 = ((1-Ohm_m_0)*(H_0))/2
    H = H_1 + H_2
    return H

def d_z_calc(a):
    d_z = (c)/((a**(2))*(H_calc(a)))
    return d_z

for x in range(0,201,1):
    z = float(x * 0.01)
    a_z = 1/(1+z)

    h = (1-a_z)/float(N)

    s = 0.5*(d_z_calc(a_z) + d_z_calc(1))


    for i in range(1,N,1):
        r = a_z + i*h

        s = s + d_z_calc(r)

    d_z = s*h

    d_L = (1+z)*d_z

    results.write(str(z) + " , " + str(d_L) + "\n")

results.close()
```

C.2 Derivation of H and q for $\alpha = 1$ modified gravity model

We start from the modified Friedmann equation

$$H^2 - \frac{H^\alpha}{r_c^{2-\alpha}} = \frac{8\pi G}{3}\rho_m, \tag{C.1}$$

for this model $\alpha = 1$ so we can re-write the modified Friedmann equation as

$$H^2 - \frac{H}{r_c} = \frac{8\pi G}{3}\rho_m, \tag{C.2}$$

considering the equation at present, H $\rightarrow H_0$ and $\rho_m \rightarrow \rho_{m,0}$, we get,

$$H_0^2 - \frac{H_0}{r_c} = \frac{8\pi G}{3}\rho_{m,0}. \tag{C.3}$$

Now, using the density parameter for matter at present,

$$\Omega_{m,0} = \frac{\rho_{m,0}}{\rho_{c,0}}, \tag{C.4}$$

we can substitute in,

$$\rho_{c,0} = \frac{3H_0^2}{8\pi G}, \tag{C.5}$$

and re-arrange to get,

$$\rho_{m,0}\frac{8\pi G}{3} = \Omega_{m,0}H_0^2, \tag{C.6}$$

substituting in this equation back into C.3 and re-arranging for r_c we get,

$$r_c = (1-\Omega_{m,0})^{-1}H_0^{-1}, \tag{C.7}$$

We can then use this equation for r_c and substitute back into C.2 and re-arranging to obtain a quadratic in terms of H,

$$H^2 - HH_0(1-\Omega_{m,0}) - \frac{8\pi G}{3}\rho_m = 0, \tag{C.8}$$

Now, using the method of completing the square to solve this quadratic to get an equation for H as a function of a,

$$\left[H-\frac{(1-\Omega_{m,0})H_0}{2}\right]^2-\frac{(1-\Omega_{m,0})^2H_0^2}{4}-\frac{8\pi G}{3}\rho_m=0, \tag{C.9}$$

Re-arranging for H,

$$H=H_0\left[\frac{(1-\Omega_{m,0})^2}{4}-\frac{8\pi G}{3H_0^2}\rho_{m,0}(\frac{a_0}{a})^3\right]^{\frac{1}{2}}+\frac{(1-\Omega)H_0}{2}, \tag{C.10}$$

Now using equation C.6 and re-arranging for $\Omega_{m,0}$ and substituting this in, we get the final expression for $H(a)$,

$$H(a)=H_0\left[\frac{(1-\Omega_{m,0})^2}{4}-\Omega_{m,0}(\frac{a_0}{a})^3\right]^{\frac{1}{2}}+\frac{(1-\Omega)H_0}{2}, \tag{C.11}$$

The deceleration parameter, q, is defined by

$$q(z)=-\frac{1}{H^2}\frac{\ddot{a}}{a}, \tag{C.12}$$

If we are to derive q into terms of a, H and dH/da we must firstly start from,

$$H=\frac{\dot{a}}{a}, \tag{C.13}$$

Substituting this into equation C.12 we get,

$$q(z)=-\frac{a\ddot{a}}{\dot{a}^2}, \tag{C.14}$$

now if we take the derivative of equation C.13,

$$\dot{H}=\frac{dH}{dt}=\frac{\ddot{a}a-\dot{a}^2}{a^2}, \tag{C.15}$$

and re-arrange for $\ddot{a}$,

$$\ddot{a}=a\left(\frac{dH}{dt}+\frac{\dot{a}^2}{a^2}\right), \tag{C.16}$$

and substitute this into equation C.14,

$$q(z) = \frac{-a^2}{\dot{a}^2}\left(\frac{dH}{dt} + \frac{\dot{a}^2}{a^2}\right), \tag{C.17}$$

We can then use the square of equation C.13, substitute this in and simplify to get,

$$q(z) = -\left(\frac{dH}{dt}\frac{1}{H^2} + 1\right), \tag{C.18}$$

but we know from chain rule that,

$$\frac{dH}{dt} = \frac{dH}{da}\frac{da}{dt} = \frac{dH}{da}\dot{a}, \tag{C.19}$$

using this and equation C.13 we can then write equation C.18 as,

$$q(z) = -\left(1 + \frac{dH}{da}\frac{a}{H}\right), \tag{C.20}$$

which gives us the deceleration parameter, q, in terms of a, H and dH/da. Now we have expressions for H in terms of a and q in terms of a, H and dH/da therefore we can derive q in terms of a using our expression of H found previously (equation C.11).
Firstly, differentiating equation C.11 with respect to a gives us,

$$\frac{dH}{da} = \frac{H_0}{2}\left(3\frac{a_0^3}{a^4}\Omega_{m,0}\right)\left(\frac{1-\Omega_{m,0}}{4} + \Omega_{m,0}\frac{a_0^3}{a^3}\right)^{-\frac{1}{2}}, \tag{C.21}$$

If we then multiply this by $\frac{a}{H}$ to give us the term seen in C.20,

$$\frac{dH}{da}\frac{a}{H} = \frac{-\frac{3}{2}\frac{a_0^3}{a^3}\Omega_{m,0}}{\left[\left(\frac{(1-\Omega_{m,0})^2}{4} + \Omega_{m,0}\frac{a_0^3}{a^3}\right)^{\frac{1}{2}} + \frac{(1-\Omega_{m,0}}{2}\right]\left[\frac{1-\Omega_{m,0}}{4} + \Omega_{m,0}\frac{a_0^3}{a^3}\right]}, \tag{C.22}$$

cancelling down and simplifying gives us,

$$\frac{dH}{da}\frac{a}{H} = \frac{-6(\frac{a_0}{a})^3\Omega_{m,0}}{(1-\Omega_{m,0})^2 + 4\Omega_{m,0}(\frac{a_0}{a})^3 + (1-\Omega_{m,0})\left[(1-\Omega_{m,0}) + 4\Omega_{m,0}(\frac{a_0}{a})^3\right]^{\frac{1}{2}}}, \tag{C.23}$$

so there plugging this expression into equation C.20,

$$q = -\left(1 + \frac{(-6(\frac{a_0}{a})^3 \Omega_{m,0})}{(1-\Omega_{m,0})^2 + 4\Omega_{m,0}(\frac{a_0}{a})^3 + (1-\Omega_{m,0})\left[(1-\Omega_{m,0}) + 4\Omega_{m,0}(\frac{a_0}{a})^3\right]^{\frac{1}{2}}}\right). \tag{C.24}$$

This is q in terms of a for the $\alpha = 1$ modified gravity model.

C.3 Proving $q < 0$

Begin with expression for $q(a)$ with $a = a_0$

$$q = -\left[1 - \frac{6\,\Omega_{m,0}}{(1-\Omega_{m,0})^2 + 4\,\Omega_{m,0} + (1-\Omega_{m,0})((1-\Omega_{m,0})^2 + 4\,\Omega_{m,0})^{1/2}}\right], \tag{C.25}$$

where $\Omega_{m,0}$ is the density parameter of matter. Now we expand the squared terms out

$$q = -\left[1 - \frac{6\,\Omega_{m,0}}{(1 - 2\,\Omega_{m,0} + \Omega_{m,0}^2 + 4\,\Omega_{m,0} + (1-\Omega_{m,0})(1 - 2\,\Omega_{m,0} + \Omega_{m,0}^2 + 4\,\Omega_{m,0})^{1/2}}\right], \tag{C.26}$$

we then eliminate the $-2\,\Omega_{m,0}$ terms and re-factorise the quadratic equations

$$q = -\left[1 - \frac{6\,\Omega_{m,0}}{(1+\Omega_{m,0})^2 + (1-\Omega_{m,0})((1+\Omega_{m,0})^2)^{1/2}}\right]. \tag{C.27}$$

Once again we expand out the brackets and find

$$q = -\left[1 - \frac{6\,\Omega_{m,0}}{\Omega_{m,0}^2 + 2\,\Omega_{m,0} + 1 + \Omega_{m,0} + 1 - \Omega_{m,0}^2 - \Omega_{m,0})}\right], \tag{C.28}$$

most terms now cancel and we are left with

$$q = -\left[1 - \frac{3\,\Omega_{m,0}}{\Omega_{m,0} + 1}\right]. \tag{C.29}$$

We now set $\Omega_{m,0} = 0.308$ (this is the value given in project document) and we find:

$$q = -0.294, \tag{C.30}$$

to 3 significant figures.

C.4 Code to Calculate the value of deceleration parameter for Modified Gravity

```
from math import pi
from math import exp
from math import inf
from math import log


results = open("qz_precition.txt","w")

results.write("z value" + " , " + "q value" + "\n")

def Calc_q(r,OM):

    k = float(r*r*r)

    q = -(1-(6*OM*k)/((1-OM)**(2)+4*OM*k+(1-OM)*((1-OM)**(2)+4*OM*k)**(1/2)))

    return q

for a in range(100,600):

    z = float(a)*0.01
    OM_m_0 = float(0.308)

    qz = Calc_q(z,OM_m_0)

    #print(str(qz))

    results.write(str(z) + " , " + str(qz) + "\n")

results.close()
```

D AGENDAS AND MINUTES

Lancaster University Department of Physics

BETA Collab Meeting

13:15 Wed 30th January, A9

AGENDA

1. **Apologies for absence**
   N/A

2. **Matters for Discussion**
   (The list things to be discussed at this meeting. These must be sent to the administrator in advance. Specific tasks can be assigned as 'actions' to individuals or groups of individuals.)

   a. *Is everyone sticking to schedule?*
   b. *Are people distributed correctly?*
   c. *What each person/subgroup has completed to date?*

Figure 17

Lancaster University Department of Physics

BETA Collab Meeting

13:00 Wednesday 30th January, A9

MINUTES

1. **Attendance List**
   All

2. **Apologies for Absence**
   N/A

3. **Minutes of previous meeting**
   N/A as this is first meeting

4. **Matters Arising**
   - *a) Part 1a task1 action: RU – taken*
   - *b) Part 1a task2 action: MG LB RU – taken*
   - *c) Part 1a task3 action: MG LB RU – taken*
   - *d) Part 2 – preliminary calculations action: AT – taken*
   - *e) Commenced research on W-first mission for Part 2b action: DB AT – taken.*

5. **Matters Discussed**
   - *a) Part 1b task1 action: MG RU LB*
   - *b) Part 1b task2 action: MG RU LB*
   - *c) Part 1b task3 action: MG RU LB*
   - *d) Part 1b task4 action: MG RU LB*
   - *e) Part 2b – coding action: DB AT*

6. **Any other business**
   Continue with tasks, subgroups of (DB AT) and (MG RU LB).

Figure 18

Lancaster University Department of Physics

BETA Collab Meeting

13:00 Wednesday 6th February, B7

AGENDA

1. **Apologies for absence**
(Members should let the Administrator know in advance if they can't make it)

No Absences.

2. **Minutes of previous meeting**
All agree.

4. **Matters for Discussion**
(The list things to be discussed at this meeting. These must be sent to the administrator in advance. Specific tasks can be assigned as 'actions' to individuals or groups of individuals.)

   a. *Look at Gant chart to assess current progress.*
   b. *Is everyone working equally?*
   c. *LaTeX report discussion.*
   d. *What tasks are completed?*
   e. *What tasks still to be commenced?*

Figure 19

Lancaster University Department of Physics

BETA Collab Meeting

13:00 Wednesday 6th February, B7

MINUTES

1. **Attendance List**
   All

2. **Apologies for Absence**
   N/A

2. **Minutes of previous meeting**
   RU and AT do task 1b and MG LB and DB moved onto 2a.
   The remaining minutes were confirmed as a true record.

4. **Matters Arising**
   a) Part 1b task1 action: RU AT – taken
   b) Part 1b task2 action: RU AT – taken
   c) Part 1b task3 action: RU AT – taken
   d) Part 1b task4 action: RU AT – taken
   e) Part 2b – coding action: DB AT – taken

5. **Matters Discussed**
   Progress report: ahead of schedule
   All of Part 1 is complete (1a and 1b)
   Part 2a is in progress
   Part 2b is complete – except Task 1.

6. **Any other business**
   a) Part 2a task1 action: DB – taken
   b) Part 2a task2 action: LB – taken
   c) Part 2a task3 action: MG DB – taken
   d) Part 2a task4 action: MG DB.
   e) Part 2b task2-7 action: AT – taken

Figure 20

Lancaster University Department of Physics

BETA Collab Meeting

13:00 Wednesday 13th February, A6

AGENDA

1. **Apologies for absence**
   (Members should let the Administrator know in advance if they can't make it)

   No Absences.

2. **Minutes of previous meeting**
   All agree.

4. **Matters for Discussion**
   (The list things to be discussed at this meeting. These must be sent to the administrator in advance. Specific tasks can be assigned as 'actions' to individuals or groups of individuals.)

   a. *Look at Gant chart to assess current progress.*
   b. *Is everyone working equally?*
   c. *Has task 5 of part 2a been successful?*
   d. *What tasks remain?*
   e. *Plan for next week, how will we tackle the last few tasks?*

Figure 21

Lancaster University Department of Physics

BETA Collab Meeting

13:00 Wednesday 13th February, A6

MINUTES

1. **Attendance List**
   All

2. **Apologies for Absence**
   N/A

2. **Minutes of previous meeting**
   Confirmed as a True Record.

4. **Matters Arising**
   a) Part 2a task 5 action: AT RU – taken
   b) Part 2a task 4 action: MG DB – taken
   c) Part 3 task 2 action: RU LB – taken
   d) Part 3 task 3 action: DB MG – in progress.

5. **Matters Discussed**
   a) Progress report: ahead of schedule
   b) Part 2a task 6 action: AT RU
   c) Part 2b task 1 action: AT.
   d) Part 3 task 1 action: AT
   e) Part 3 task 4 action: DB
   f) Part 3 task 5 and 6: AT RU
   g) Report rough draft in progress
   h) Equations/derivations started being implemented in LaTeX: action LB
   i) Part 2a task 2: Still needs completing, action: LB

6. **Any other business**
   Attached in the email are the objectives for the report…
   Use these points as a guide for creating the Report in the next few weeks.

Figure 22

Lancaster University Department of Physics

BETA Collab Meeting

13:00 Wednesday 20th February, County South

AGENDA

1. **Apologies for absence**
   (Members should let the Administrator know in advance if they can't make it)

   No Absences.

2. **Minutes of previous meeting**
   All agree.

4. **Matters for Discussion**
   (The list things to be discussed at this meeting. These must be sent to the administrator in advance. Specific tasks can be assigned as 'actions' to individuals or groups of individuals.)

   a. *Plan Report and Discuss plan for last week of lab as we have Completed all necessary tasks.*
   b. *Each member collate their completed tasks and organise ready for report write up.*
   c. *Refine written sections so they're to a high standard.*

Figure 23

Lancaster University Department of Physics

BETA Collab Meeting

13:00 Wednesday 20th February, County South

MINUTES

1. Attendance List
All

2. Apologies for Absence
N/A

2. Minutes of previous meeting
Confirmed as a True Record.

4. Matters Arising
a) All tasks have been completed
b) Graphs uploaded to Box account, action: Taken
c) Report Layout discussed
d) Delegate sections of the report to individuals.

5. Matters Discussed
a) Progress report: Tasks Completed 100%
b) Each member of group to gather their completed tasks from the project and prepare the necessary information for the report.

6. Any other business

Figure 24

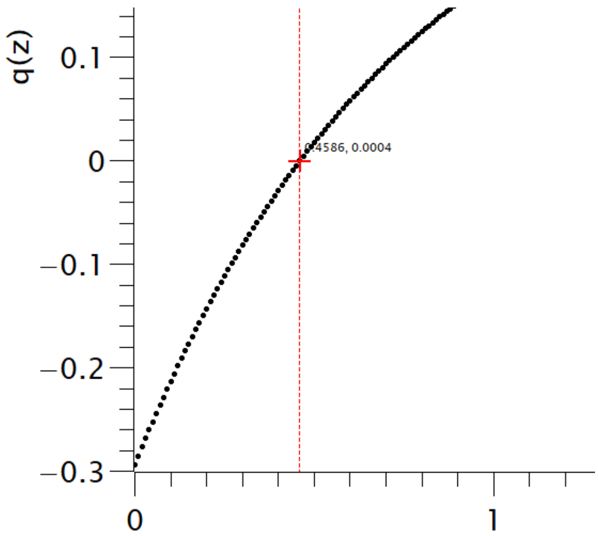

Figure 25: Close up of the z value at q(z) = 0, extracted using data analysis on QTI plot.

	zvalue[X1]	z[X2]	q(z)[Y2]
34	1.33	0.33	-0.064822139...
35	1.34	0.34	-0.059393260...
36	1.35	0.35	-0.054039781...
37	1.36	0.36	-0.048760575...
38	1.37	0.37	-0.043554522...
39	1.38	0.38	-0.038420511...
40	1.39	0.39	-0.033357443...
41	1.4	0.4	-0.028364227...
42	1.41	0.41	-0.023439783...
43	1.42	0.42	-0.018583044...
44	1.43	0.43	-0.013792953...
45	1.44	0.44	-0.009068465...
46	1.45	0.45	-0.004408550...
47	1.46	0.46	0.0001878129...
48	1.47	0.47	0.0047216300...
49	1.48	0.48	0.0091938944...

Figure 26: Closest values to q(z) = 0 in table of data and the corresponding z values.

REFERENCES

[1] White Dwarfs and The Age of the Universe. Vanderbilt University.

[2] Elizabeth Howell. Globular Clusters. SPACE. 2015.

[3] S.Moehler and G.Bono. White Dwarfs in Globular Clusters. 2011.

[4] Martin White. Baryon Acoustic Oscillations: A standard ruler method for determining the expansion rate of the Universe. UC Berkeley/LBNL. 2005.

[5] Daniel J. Eisenstein *et al*, Detection of the Baryon Acoustic Peak in the large-scale correlation function of SDSS luminous red galaxies, The astrophysical Journal, 2004, arXiv:astro-ph/0501171

[6] Dvali Gia and Turner Michael. Dark Energy as a Modification of The Friedmann Equation. 2003

[7] ESA Science and Technology. Key Milestone for Euclid Mission, Now Ready For Final Assembly. ESA. 2018.

[8] R. Laureijs *et al*, EUCLID, Mapping the geometry of the dark Universe, 2011, arXiv:1110.3193 [astro-ph.CO].

[9] Hogg David. Distance Meaures in Cosmology. 2000.

[10] Dimitar Ivanov, Stefano Liberati, Matteo Viel, and Matt Visser. Non-perturbative results for the luminosity and area distances. 2018.

[11] S. Tsujikawa, Quintessence: A Review, 2013, arXiv:1304.1961 [gr-qc].

[12] J. B. Durrive, J. Ooba, K. Ichiki, N. Sugiyama, Updated observational constraints on quintessence dark energy models, 2018, arXiv:1801.09446 [astro-ph.CO].

[13] Krauss Lawrence. Space, Time, and Matter: Cosmological Parameters.Case Western Reserve University. 2000.

[14] Edward L. Wright. Listening for the size of the Universe. 2014.

[15] D. Spergel *et al.*,Wide-Field InfraRed Survey Telescope-Astrophysics Focused Telescope Assets WFIRST-AFTA Final Report,2013, arXiv:1305.5422 [astro-ph.IM].

[16] Ethan Siegel, How is the Universe bigger than its age?, 2014.